141

[redacted]

Copy 41

[redacted]

NASA Project Apollo Working Paper No. **1040**

PROJECT APOLLO

STATIC LONGITUDINAL STABILITY CHARACTERISTICS OF A MODIFIED ATMOSPHERIC ABORT CONFIGURATION FOR PROJECT APOLLO

CLASSIFICATION CHANGED TO
UNCLASSIFIED
BY AUTHORITY OF SCG-11-1
DATE 1 January 1966

[redacted]

NATIONAL AERONAUTICS AND SPACE ADMINISTRATION

MANNED SPACECRAFT CENTER

Langley Air Force Base, Va.

December 20, 1961

[redacted]

N66-25886 (ACCESSION NUMBER)
(THRU)
59 (PAGES)
1002 (CODE)
TMX 53290 (NASA CR OR TMX OR AD NUMBER)
(CATEGORY)
FACILITY FORM 602

[redacted]

NASA PROJECT APOLLO WORKING PAPER NO. 1040

PROJECT APOLLO

STATIC LONGITUDINAL STABILITY CHARACTERISTICS OF A MODIFIED ATMOSPHERIC ABORT CONFIGURATION FOR PROJECT APOLLO

Prepared by: Robert H. Moore, Jr.

Robert H. Moore, Jr.
Engineering Technician (General)

Authorized for Distribution:

for Paul E. Purser
Robert R. Gilruth, Director

CLASSIFICATION CHANGED TO

BY AUTHORITY OF

DATE

NATIONAL AERONAUTICS AND SPACE ADMINISTRATION

MANNED SPACECRAFT CENTER

Langley Air Force Base, Va.

December 20, 1961

[redacted]

[redacted]

TABLE OF CONTENTS

Section	Page
SUMMARY	1
INTRODUCTION	1
SYMBOLS	2
MODEL	3
TEST FACILITIES, RANGES AND ACCURACIES	4
PRESENTATION OF RESULTS	4
DISCUSSION	4
Abort Configuration Without the Conical Shroud	4
Abort Configuration With the Conical Shroud	6
CONCLUSIONS	7
REFERENCE	8
TABLES I to II	9 to 10
FIGURES 1 to 9	11 to 54

[redacted]

[redacted]

LIST OF TABLES

Table		Page
I	Test Conditions	9
II	Accuracy of Data	10

[redacted]

LIST OF FIGURES

Figure		Page
1	Sketch showing stability axis system used	11
2	Sketch of Apollo atmospheric abort configuration tested showing general dimensions	12
3	Photographs of the test configuration	13
4	Aerodynamic characteristics of the atmospheric abort configuration without conical shroud around rocket nozzles at Mach numbers from 0.3 to 1.20	15
5	Aerodynamic characteristics of the atmospheric abort configuration without the conical shroud around rocket nozzles at Mach numbers from 1.46 to 2.16	24
6	Aerodynamic characteristics of the atmospheric abort configuration with the conical shroud around rocket nozzles at Mach numbers from 0.3 to 1.20	33
7	Aerodynamic characteristics of the atmospheric abort configuration with the conical shroud around rocket nozzles at Mach numbers from 1.46 to 2.16	42
8	Effect of center-of-gravity location of the longitudinal stability characteristics of the atmospheric abort configuration without conical shroud around rocket nozzles	51
9	Effect of center-of-gravity location of the longitudinal stability characteristics of the atmospheric abort configuration with conical shroud around rocket nozzles	53

[redacted]

STATIC LONGITUDINAL STABILITY CHARACTERISTICS OF A MODIFIED ATMOSPHERIC ABORT CONFIGURATION FOR PROJECT APOLLO

SUMMARY

A preliminary investigation at Mach numbers from 0.3 to 2.16 has been conducted in the NASA Langley Research Center 8-foot transonic pressure tunnel and the Langley Unitary Plan wind tunnel to determine the static longitudinal stability characteristics of a Project Apollo modified atmospheric abort configuration. These modifications were an increase in the rocket fineness ratio from 5.85 to 8.61, and a change in the command module afterbody angle from 35° to 33°. The configuration was tested with and without a conical shroud, or fairing, around the abort rocket nozzles.

The pitching-moment data was reduced about five center-of-gravity locations. The results indicate that the configuration without the conical shroud is unstable throughout the Mach number range, except for the two most forward center-of-gravity locations. Only the most forward moment center would be considered satisfactory and represents the addition of a large amount of ballast to the rocket nose. The data also shows a discontinuity in the pitching-moment coefficient near Mach number of 1.57. This discontinuity is probably associated with the unsteady flow separation around the exposed rocket nozzles. The configuration tested with the conical shroud indicated the configuration to be fairly stable throughout the Mach number range, except for the most rearward center-of-gravity location. This instability is due primarily to the large axial-force coefficient acting on the vertically displaced center of gravity. The data with the conical shroud indicates a large reduction in the discontinuity in the pitching-moment coefficient shown for the configuration without the conical shroud.

INTRODUCTION

Tests were made on a representative Apollo atmospheric abort configuration similar to that reported in reference 1. The data in reference 1 indicated there were two problem areas:

(a) A lack of stability near a Mach number of 1.00 which would require a large amount of ballast added to the front of the abort rocket to make the configuration stable.

[redacted]

(b) Data also showed a discontinuity at low angles of attack in the pitching-moment data near M = 1.57.

Two modifications were made to the reference 1 basic abort configuration. The rocket fineness ratio was increased in an attempt to increase the stability characteristics of the configuration, also the afterbody angle was decreased from 35° to 33° in order to obtain more workable volume in the command module. It was felt that the low angle-of-attack discontinuity was associated with the unsteady flow separation around the exposed rocket nozzles. Unpublished results of tests made in the Langley Unitary Plan wind tunnel on the C-1 Apollo launch configuration indicated that a conical shroud around the abort rocket nozzles eliminated the discontinuity in the pitching-moment data near M = 1.57. Tests were made both with and without such a device on the abort configuration at both transonic and supersonic speeds. The tests were conducted in the Langley 8-foot transonic pressure tunnel and the Langley Unitary Plan wind tunnel through a Mach number range from 0.3 to 2.16. The purpose of this paper is to report the results of these tests.

SYMBOLS

Data are presented using both the body and stability systems of axes. The body system of axis is shown in figure 1. The symbols and coefficients used in this paper are defined as follows:

C_A axial-force coefficient, $\frac{\text{Total axial force}}{qS}$

C_D drag coefficient, $C_A \cos \alpha + C_N \sin \alpha$

C_L lift coefficient, $C_N \cos \alpha - C_A \sin \alpha$

C_m pitching-moment coefficient, $\frac{\text{Pitching moment}}{qSd}$

C_{L_α} lift-curve slope per degree, $\frac{\partial C_L}{\partial \alpha}$

C_{m_α} normal-force curve slope per deg, $\frac{\partial C_m}{\partial \alpha}$

D reference dimension (maximum model dia.), ft

M	free-stream Mach number
p	free-stream static pressure, lb/sq ft
q	free-stream dynamic pressure, $0.7\ pM^2$, lb/sq ft
R	Reynolds number based on maximum diameter
S	reference area, $\frac{\pi}{4}D^2$, sq ft
$\frac{X}{D}$	longitudinal location of the center of gravity from heat-shield face
$\frac{Z}{D}$	vertical location of the center of gravity
α	angle of attack of model center line, deg
c.g.	center-of-gravity location

Subscript:

t	trim angle of attack

MODEL

General dimensions of the configuration tested are given in figure 2. The test model was made of stainless steel and aluminum. The capsule had a maximum diameter of D = 10.92 inches; the heat-shield radius was 1.2D and the corner radius was 0.05D.

The atmospheric abort configuration is basically the same as the long tower configuration of reference 1, except for the following changes:

(a) Afterbody angle changed from 35° to 33°

(b) The rocket fineness ratio was increased

In order to obtain the test information through the angle-of-attack range presented for the transonic data, it was necessary to test the model through two incremental angle-of-attack ranges. This was done by the use of two sting-to-balance adapters; the two adapters allowed testing in the following angle-of-attack ranges:

(a) 0° adapter - α -4° to 25°

(b) 40° adapter - α 25° to 50°

TEST FACILITIES, RANGES AND ACCURACIES

The tests were conducted in the Langley 8-foot transonic pressure tunnel over a Mach number range from 0.3 to 1.20, and in the Langley Unitary Plan wind tunnel at Mach numbers 1.46, 1.50, 1.57, 1.80, and 2.16.

Table I shows the test conditions for the atmospheric abort configuration. Table II shows the accuracy range of the data obtained from these tests. Two sets of values are given in tables I and II for the transonic data because it was necessary to lower the dynamic pressure at the higher angles of attack, in order not to exceed the balance design loads.

PRESENTATION OF RESULTS

The basic data for the atmospheric abort configuration with and without the conical shroud are given in figures 4 to 7. The basic moment data for the configuration were calculated for five center-of-gravity locations. The basic results are summarized in figures 8 and 9.

DISCUSSION

The static longitudinal stability data presented in this paper are the results of a wind-tunnel investigation of a modified Apollo atmospheric abort configuration with and without the conical shroud around the exposed rocket nozzles through the Mach number range from 0.3 to 2.16.

Abort Configuration Without the Conical Shroud

The basic data for the configuration without the conical shroud are presented in figures 4 and 5. The basic moment data in figures 4 and 5 have been reduced about five center-of-gravity locations as shown in figure 2. The different centers of gravity were used in an attempt to determine the amount of ballast needed to make the configuration stable through the Mach number range. Four of the center-of-gravity

locations shown were not on the axis of symmetry. This vertical offset is the result of the offset center of gravity associated with the reentry configuration. The center-of-gravity locations about which the moment data are presented were obtained by considering three components: the reentry body, the tower-mounted rocket case, and ballast added to the rocket nose. The condition of no ballast gives the most rearward center of gravity and corresponds to the condition at the end of the abort rocket burning as shown on the model sketch of figure 2.

Three of the other center-of-gravity locations, as summarized in the table in figure 2, were then obtained by adding equal increments of ballast to the rocket nose. For comparison, data are presented about a moment center on the axis of symmetry for the most rearward moment center location which is $\frac{X}{D} = 0.390$, $\frac{Z}{D} = 0$.

The data presented in figure 4 are the transonic data through the Mach number range of 0.3 to 1.20 only. The data presented in figure 4(e) $\left(\frac{X}{D} = 0.39, \frac{Z}{D} = 0\right)$ show the configuration to be neutrally stable throughout the angle-of-attack range. Figure 4(f) $\left(\frac{X}{D} = 0.39, \frac{Z}{D} = -0.0473\right)$ shows the configuration to be very unstable throughout the Mach number and angle-of-attack range tested ($M = 0.3$ to $M = 1.20$ and $\alpha = -4^{\circ}$ to $+50^{\circ}$). An increase in ballast in the rocket nose shows the configuration to be unstable still, as presented in figure 4(g) $\left(\frac{X}{D} = 0.507, \frac{Z}{D} = -0.0444\right)$. A more forward shift in the center of gravity will make the configuration stable over a limited angle-of-attack range of about $\alpha = 10^{\circ}$ to 26° with trim angle of about 11° at $M = 1.03$. These data are presented in figure 4(h) $\left(\frac{X}{D} = 0.611, \frac{Z}{D} = -0.0427\right)$. The most forward shift in the moment center as shown in figure 4(i) $\left(\frac{X}{D} = 0.706, \frac{Z}{D} = -0.0407\right)$, gives good stability over a fairly large angle range ($\alpha = 2^{\circ}$ to 50° at $M = 0.8$) and trim angle of about 2°. Only the stability shown in figure 4(i) for the most forward condition would be considered satisfactory; however, this represents the addition of a large amount of ballast.

The supersonic data for the configuration without the conical shroud are presented in figure 5, and show the configuration to be stable over a limited angle-of-attack range throughout the Mach number range; except for the $\frac{X}{D} = 0.390$, $\frac{Z}{D} = -0.0473$ moment center location.

This was not unexpected as the vertical offset tends to make the configuration unstable due to the rather large destability moment associated with the axial-force coefficient. These data also show a discontinuity in the moment coefficient data near M = 1.57, which is felt to be due to the unsteady flow separation around the exposed rocket nozzles. This discontinuity in the pitching-moment coefficient data is similar to that which occurred in the data of reference 1.

Summary data for the configuration without the conical shroud are presented in figure 8. These data show a reduction in the trim drag coefficient near M = 1.57 similar to that shown in the data of reference 1. The data also show that the moment center of $\frac{X}{D} = 0.507$, $\frac{Z}{D} = -0.0444$ is marginally stable at M = 1.03 with a rather large trim angle; however, only the most forward center-of-gravity location provides satisfactory stability characteristics over the Mach number range.

The results presented in this paper for the basic configuration are generally similar to the data reported in reference 1. It is felt since the data are similar, any improvement in stability due to the increase of the rocket fineness ratio was counteracted by a decrease in stability due to the change in afterbody angle.

Abort Configuration With the Conical Shroud

The abort configuration with the conical shroud was tested in an effort to improve the stability of the configuration and to eliminate or lessen the discontinuity near M = 1.57 due to the unsteady flow separation around the exposed rocket nozzles. Unpublished data obtained in the Langley Unitary Plan wind tunnel showed that a conical shroud or fairing around the rocket nozzles eliminated the discontinuity in the pitching-moment data at M = 1.57 for the C - 1 booster-capsule-tower configuration.

The basic data for the configuration with the conical shroud are presented in figures 6 and 7, and the summary data are presented in figure 9. Since the moment data are quite nonlinear, the pitching-moment curve slope does not always give a true indication of the stability of the configuration. Comparison of the basic data as well as the summary data indicate that the addition of the conical shroud provides a margin of positive stability for all moment centers, except $\frac{X}{D} = 0.390$, $\frac{Z}{D} = -0.0473$. This is due mainly to the large axial-force coefficient acting on the vertical displaced center of gravity. It is felt that considerable saving in ballast can be obtained with the location of the vertical offset moment center closer to the axis of

symmetry. A large amount of ballast is still required to obtain satisfactory stability characteristics with this configuration; however, the shape of this C_m vs α curve is much better with the shroud. The basic supersonic data with the shroud presented in figure 7, and compared with the basic supersonic data without the shroud presented in figure 5, show that the discontinuity near M = 1.57 is nearly eliminated.

CONCLUSIONS

The results of a preliminary investigation of a modified atmospheric abort configuration with and without the conical shroud indicate the following:

1. The configuration without the conical shroud requires the addition of a very large amount of ballast to provide satisfactory stability characteristics.

2. The addition of the conical shroud improves the stability of the configuration through the Mach number range; however, a large amount of ballast is still required to provide satisfactory stability characteristics.

3. The configuration with the conical shroud shows a large reduction in the discontinuity near M = 1.57.

4. Considerable savings in ballast could be obtained through shifting the vertical center of gravity closer to the axis of symmetry.

[redacted]

REFERENCE

1. Jackson, Bruce G., and Moseley, William C., Jr.: Project Apollo - Static Longitudinal Stability Characteristics of a Blunt Symmetrical Reentry Configuration and a Tower-Mounted Rocket Atmospheric Abort Configuration Which Meet the Apollo Mission Requirements. NASA Project Apollo Working Paper No. 1022, Jul. 19, 1961.

[redacted]

TABLE I. - TEST CONDITIONS

Facility	Mach number	Stagnation pressure lb/sq in. abs		Dynamic pressure lb/sq ft		Stagnation temperature °F	Reynolds number[1]	
Langley 8-foot transonic pressure tunnel	0.3	14.7	14.7	125	125	121	1.65×10^6	1.65×10^6
	.5	14.7	13.3	311	283	121	2.50×10^6	2.30
	.7	14.7	10.5	521	374	121	3.17	2.33
	.8	14.7	9.8	619	414	121	3.44	2.32
	.9	14.7	9.3	706	448	121	3.60	2.30
	.95	14.7	8.9	745	463	121	3.70	2.32
	1.00	14.7	8.9	783	476	121	3.75	2.31
	1.03	14.7	8.9	803	484	121	3.75	2.33
	1.15	14.7	8.9	864	519	121	3.85	2.34
	1.20	14.7	8.9	882	530	121	3.85	2.34
Langley Unitary Plan wind tunnel	1.46	6.0		372		125	1.66×10^6	
	1.50	6.0		372		125	1.89	
	1.57	7.0		427		125	1.89	
	1.80	8.0		453		125	1.99	
	2.16	10.0		468		125	2.14	

[1]Based on capsule diameter.

TABLE II.- ACCURACY OF DATA

Facility	Mach number	Accuracy of -											
		M	α_y, deg	C_m		C_N		C_A		C_L		C_D	
Langley 8-foot transonic pressure tunnel	0.3	±0.005	±0.2	±0.008	±0.008	±0.043	±0.043	±0.043	±0.043	±0.043	±0.043	±0.043	±0.043
	.5	±.005	±.2	±.003	±.004	±.017	±.019	±.017	±.019	±.017	±.019	±.017	±.019
	.7	±.005	±.2	±.002	±.003	±.010	±.014	±.010	±.014	±.010	±.014	±.010	±.014
	.8	±.005	±.2	±.002	±.003	±.009	±.013	±.009	±.013	±.009	±.013	±.009	±.013
	.9	±.005	±.2	±.001	±.002	±.008	±.012	±.008	±.012	±.008	±.012	±.008	±.012
	.95	±.005	±.2	±.001	±.002	±.007	±.012	±.007	±.012	±.007	±.012	±.007	±.012
	1.00	±.005	±.2	±.001	±.002	±.007	±.011	±.007	±.011	±.007	±.011	±.007	±.011
	1.03	±.005	±.2	±.001	±.002	±.007	±.011	±.007	±.011	±.007	±.011	±.007	±.011
	1.15	±.005	±.2	±.001	±.002	±.006	±.010	±.006	±.010	±.006	±.010	±.006	±.010
	1.20	±.005	±.2	±.001	±.002	±.006	±.010	±.006	±.010	±.006	±.010	±.006	±.010
Langley Unitary Plan wind tunnel	1.46	±0.015	±0.1	±0.00057		±0.0062		±0.0062		±0.0062		±0.0062	
	1.50	±.015	±.1	±.00057		±.0062		±.0062		±.0062		±.0062	
	1.57	±.015	±.1	±.00049		±.0054		±.0054		±.0054		±.0054	
	1.80	±.015	±.1	±.0049		±.0054		±.0054		±.0054		±.0054	
	2.16	±.015	±.1	±.0045		±.0049		±.0049		±.0049		±.0049	

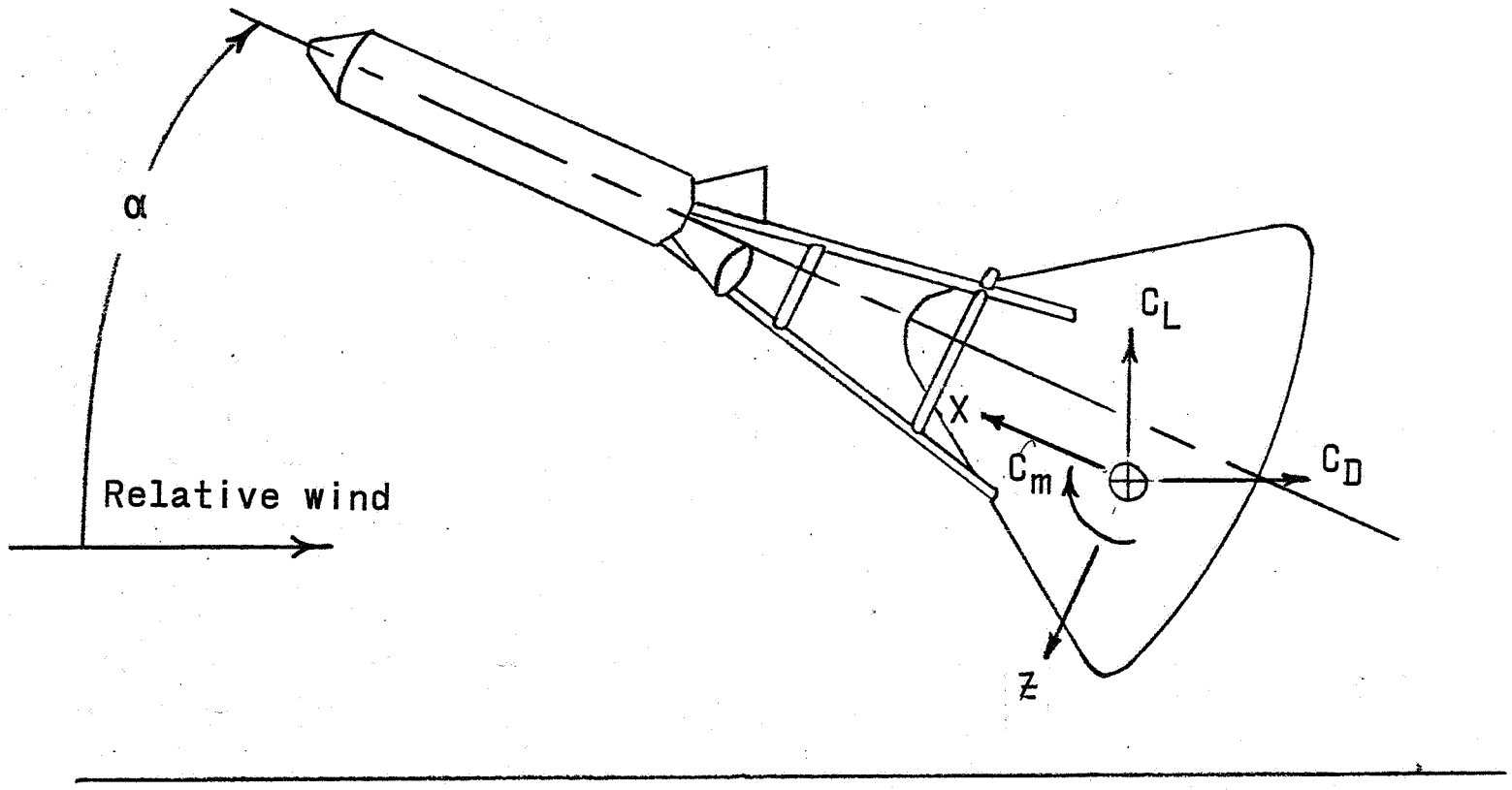

Figure 1.- Sketch showing stability axis system used.

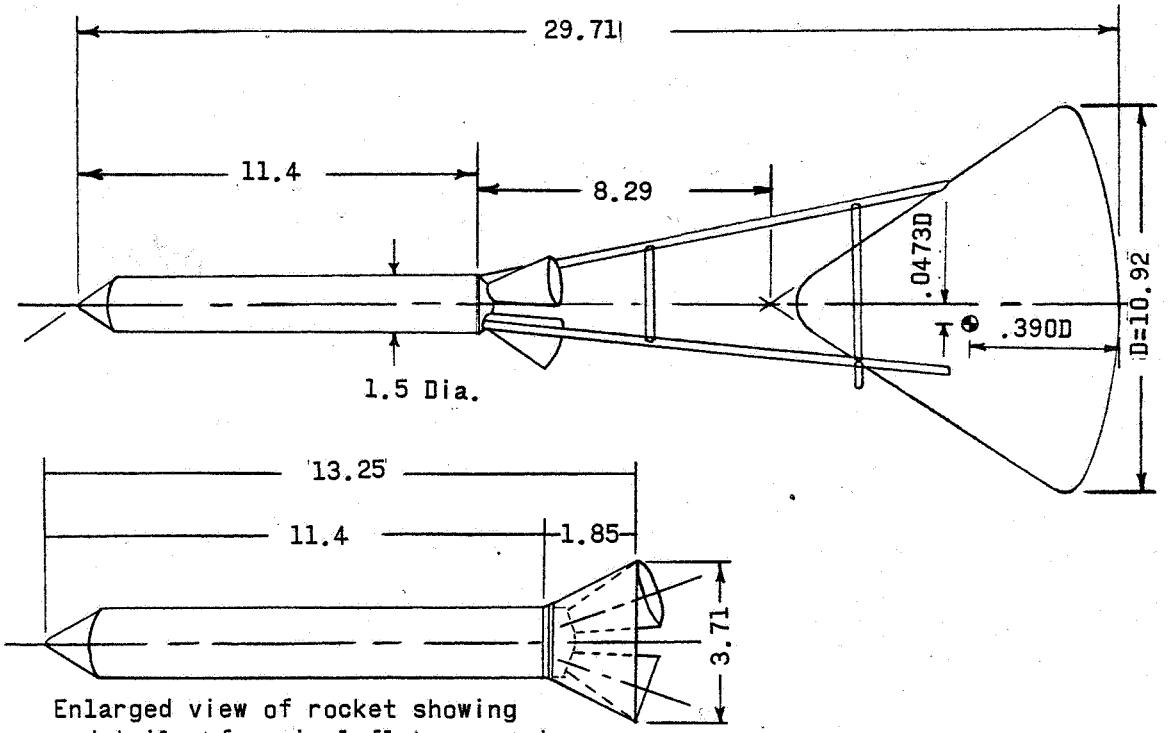

Enlarged view of rocket showing details of conical flare around rocket nozzles.

MOMENT CENTERS	X/D	Z/D
○	0.390	0.0
□	0.390	0.0473
◇	0.507	0.0444
△	0.611	0.0427
◺	0.706	0.0407

Figure 2.- Sketch of Apollo atmospheric abort configuration tested showing general dimensions. (All dimensions in inches)

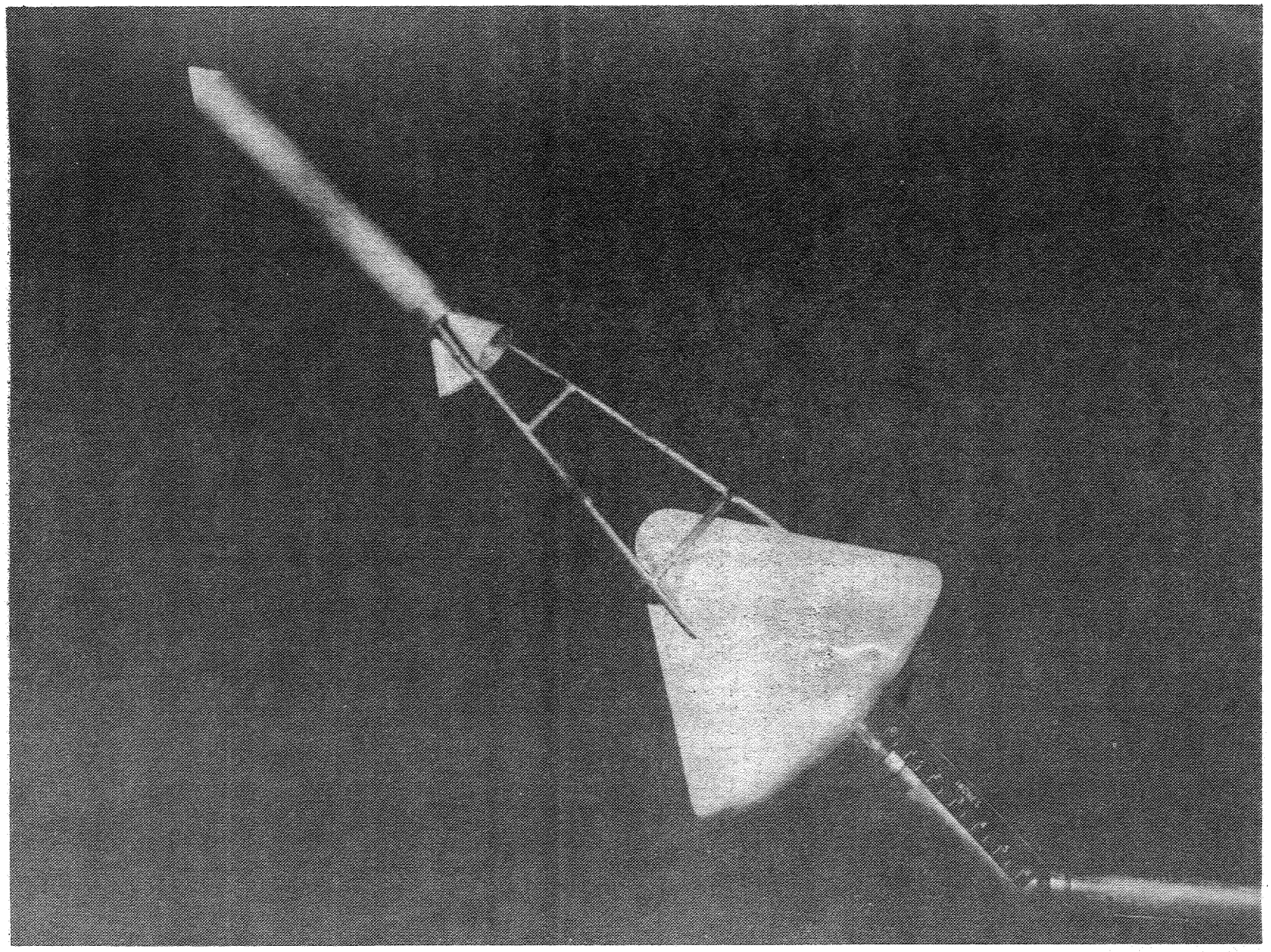

(a) Without conical shroud.

Figure 3.- Photographs of the test configuration.

CONFIDENTIAL

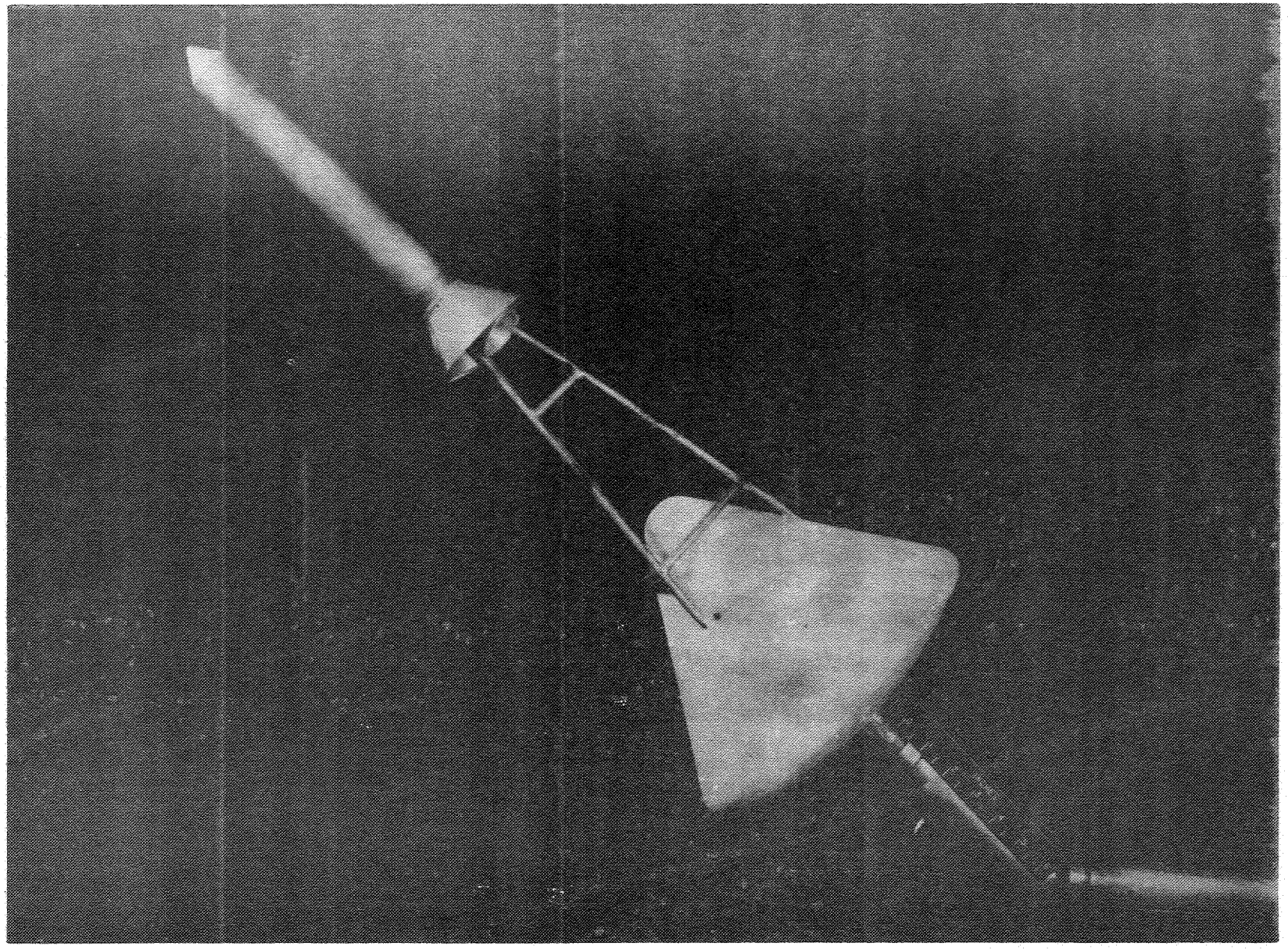

(b) With conical shroud.

Figure 3.- Concluded.

CONFIDENTIAL

[redacted]

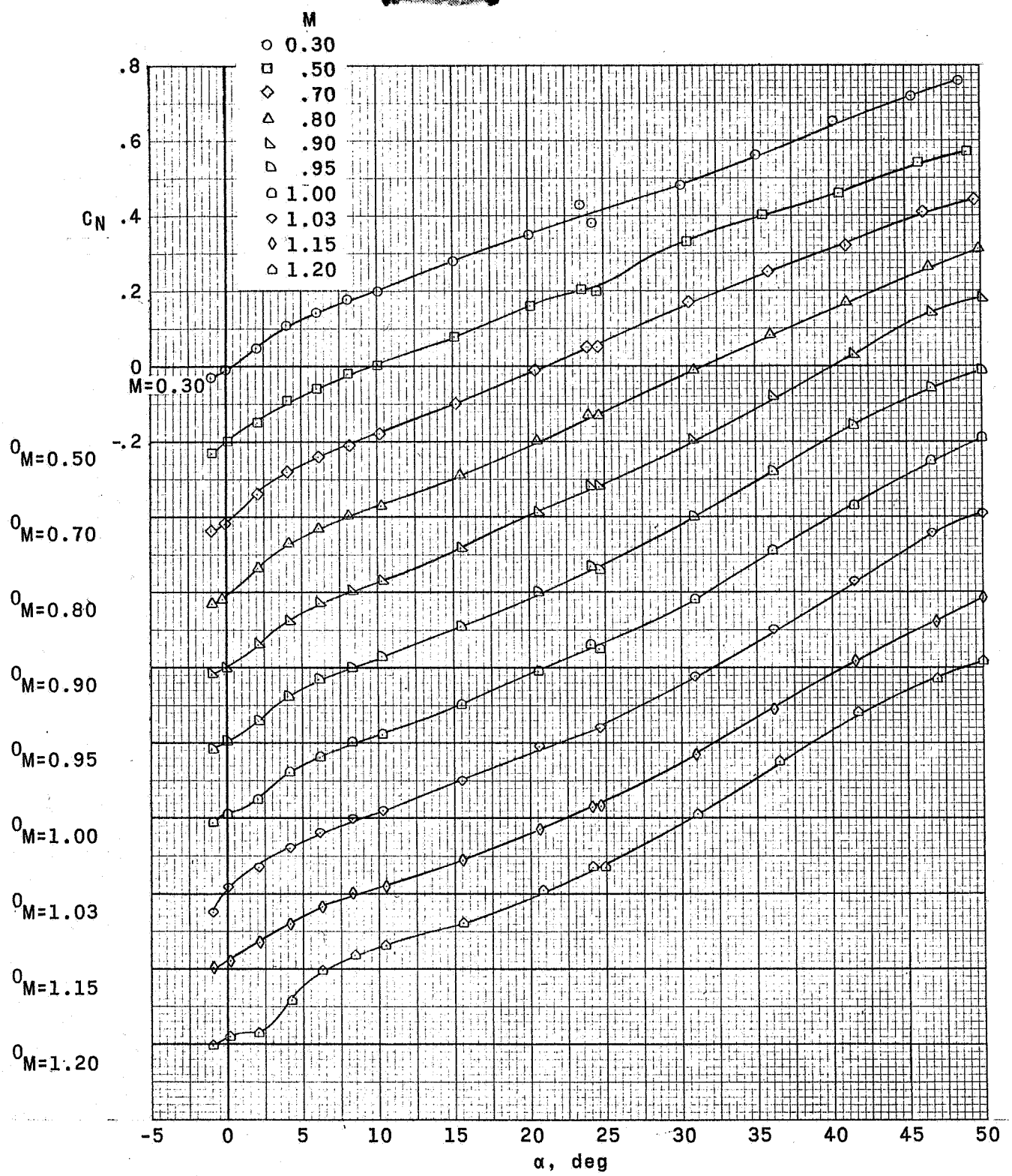

(a) Normal-force coefficient.

Figure 4.- Aerodynamic characteristics of the atmospheric abort configuration without conical shroud around rocket nozzles at Mach numbers from 0.3 to 1.20.

[redacted]

[redacted]

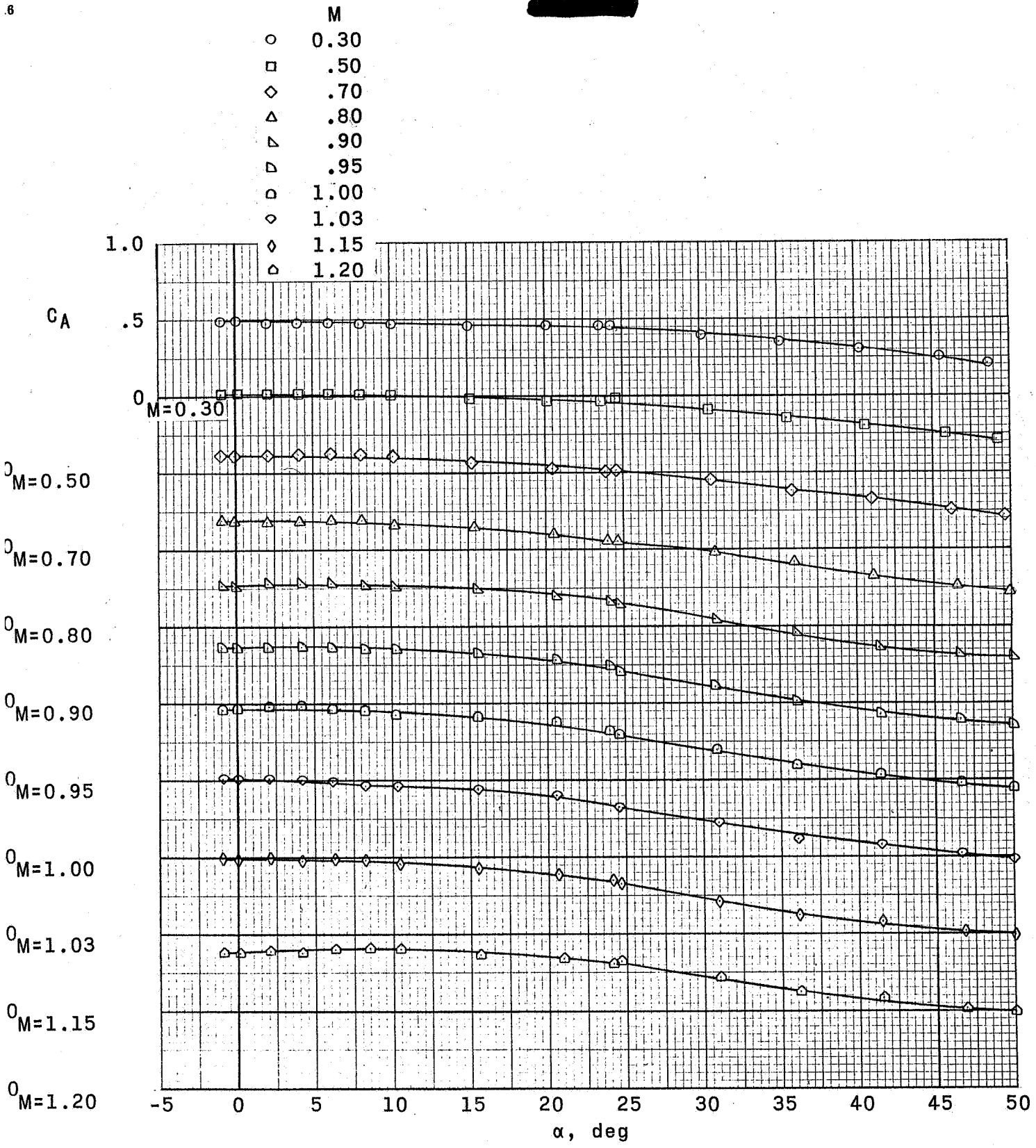

(b) Axial-force coefficient.

Figure 4.- Continued.

[redacted]

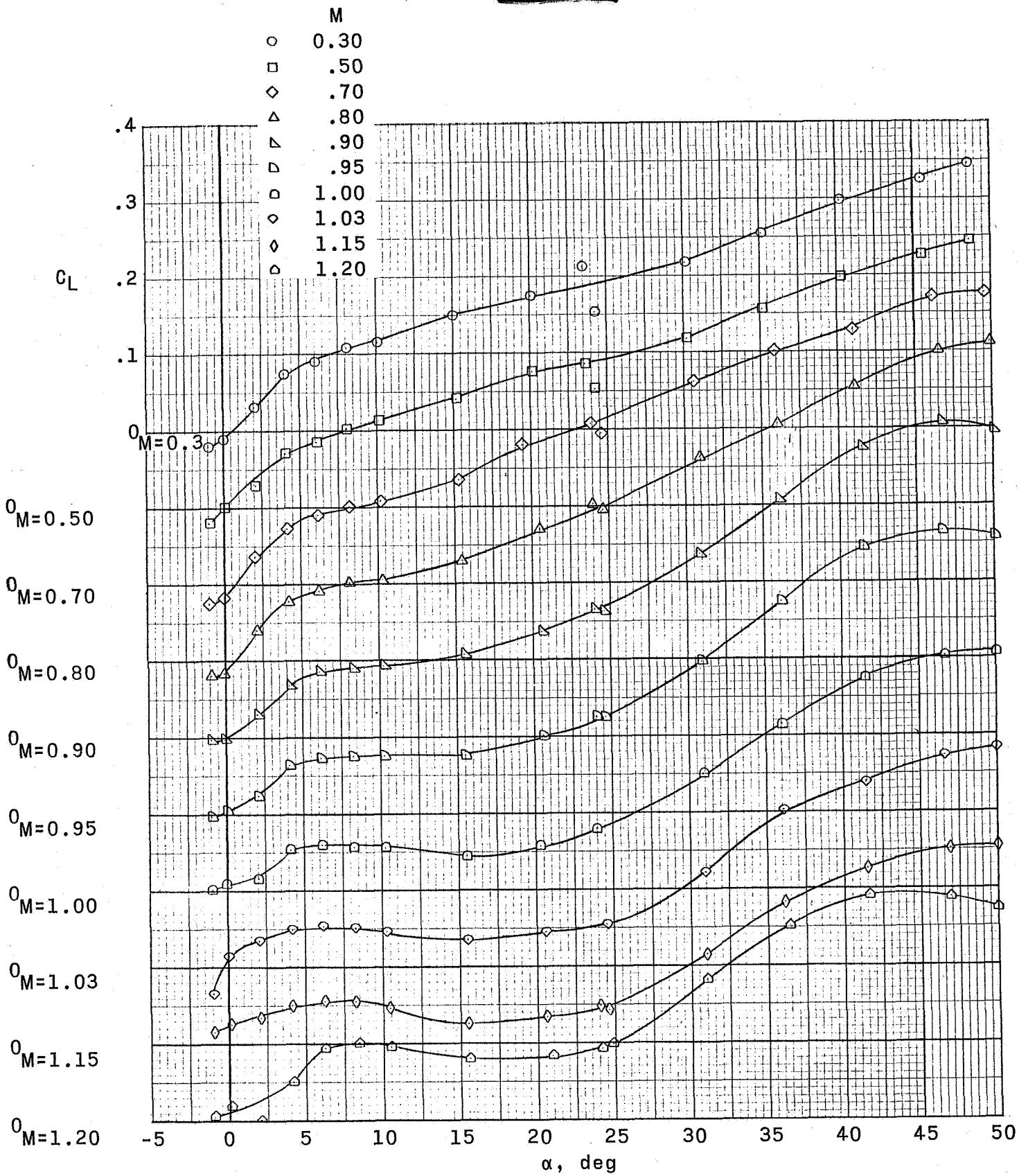

(c) Lift coefficient.

Figure 4.- Continued. [redacted]

[redacted]

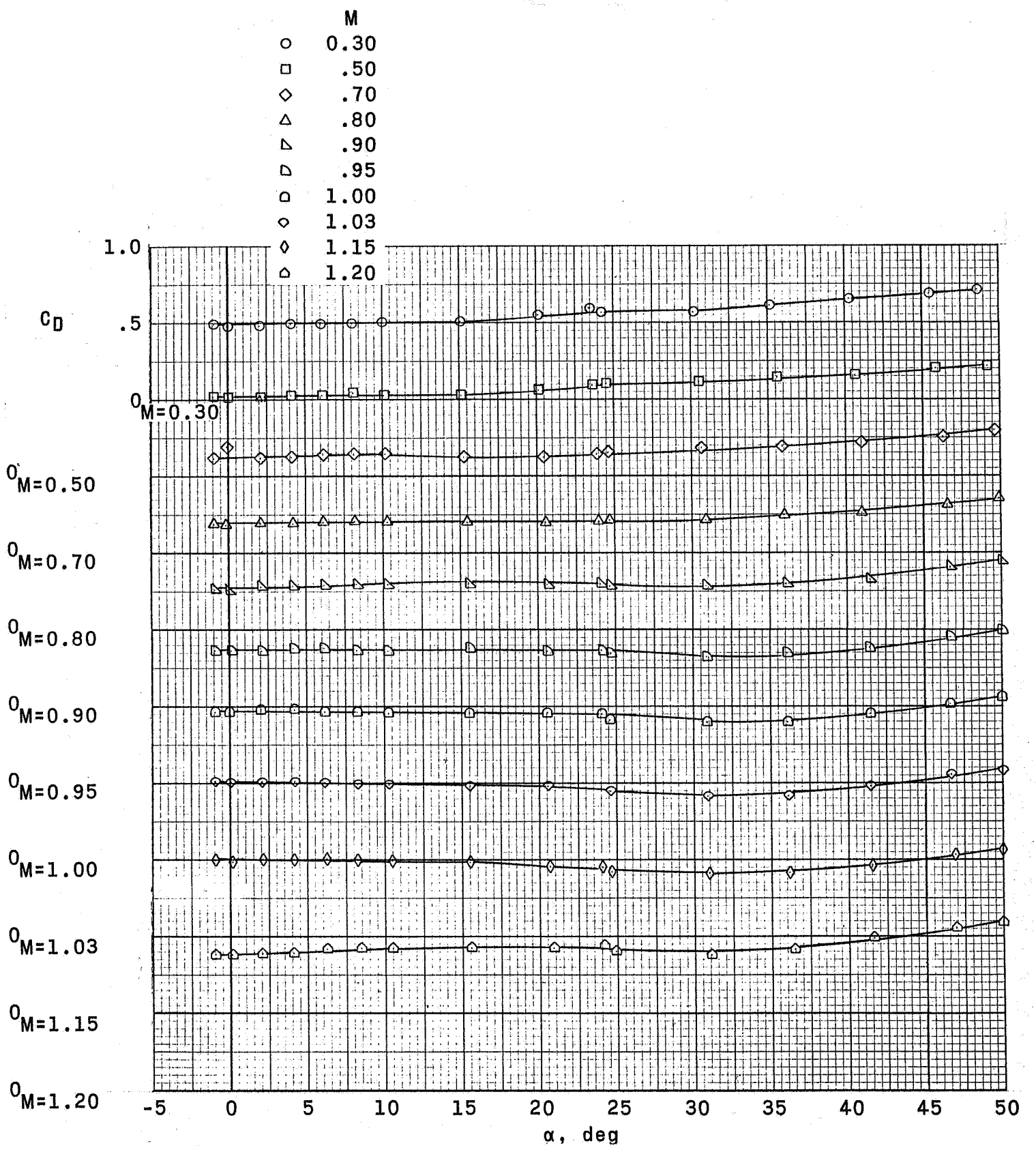

(d) Drag coefficient.

Figure 4.- Continued. [redacted]

[redacted]

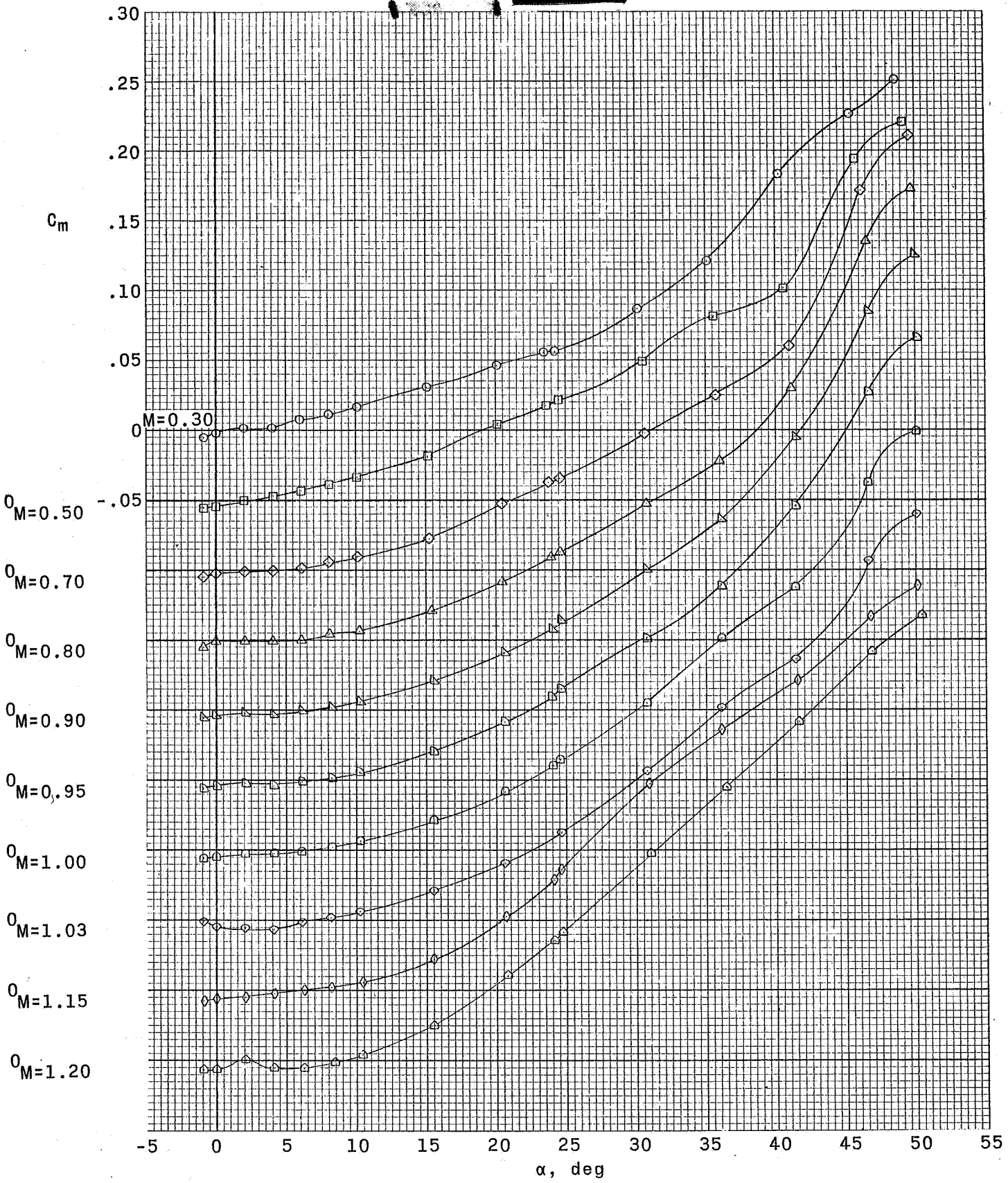

(e) Pitching-moment coefficient.
c.g. = X/D = 0.390 Z/D = 0.000

Figure 4.- Continued.

[redacted]

[redacted]

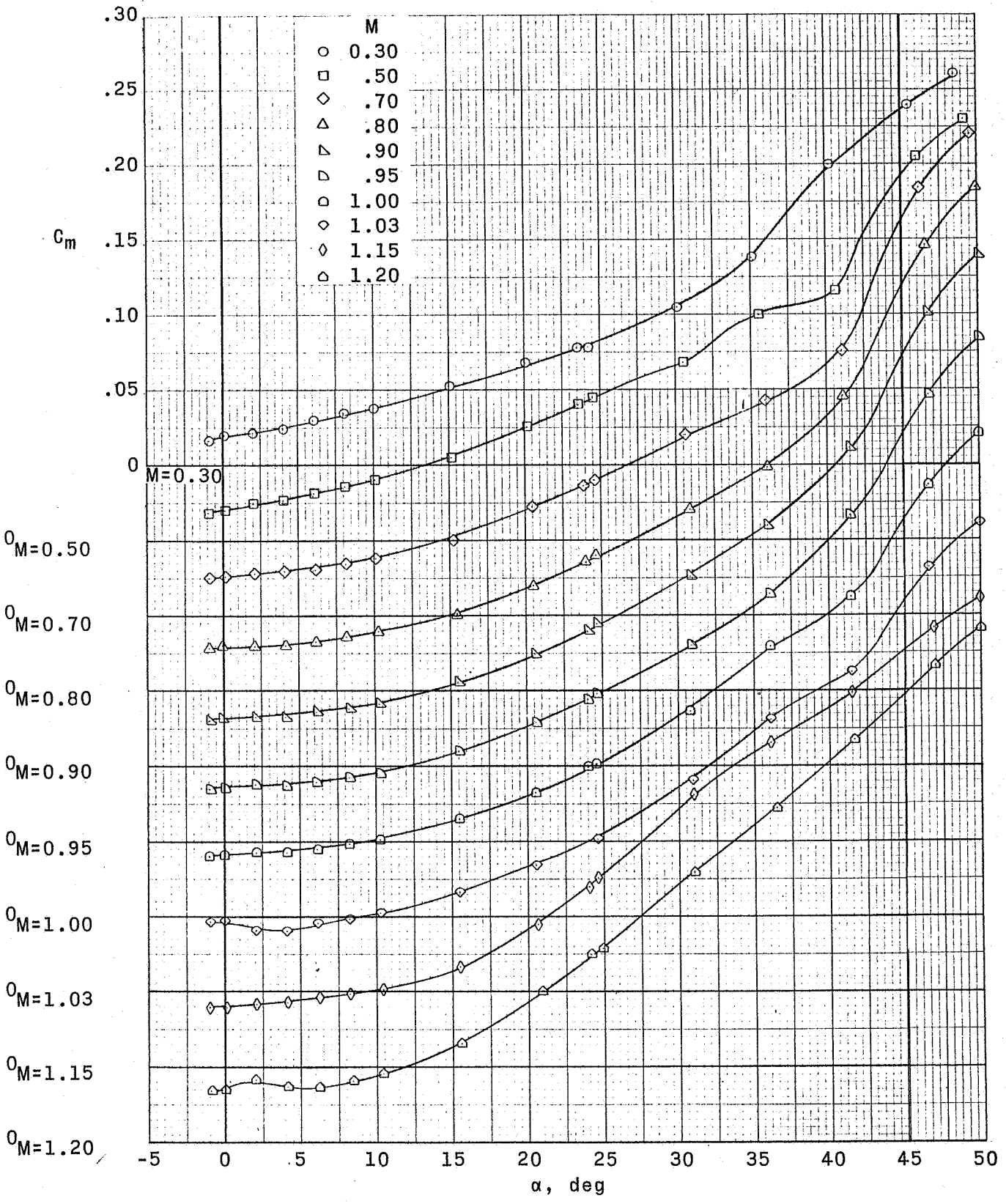

(f) Pitching-moment coefficient.
c.g. = X/D = 0.390 Z/D = 0.0473

Figure 4.- Continued. [redacted]

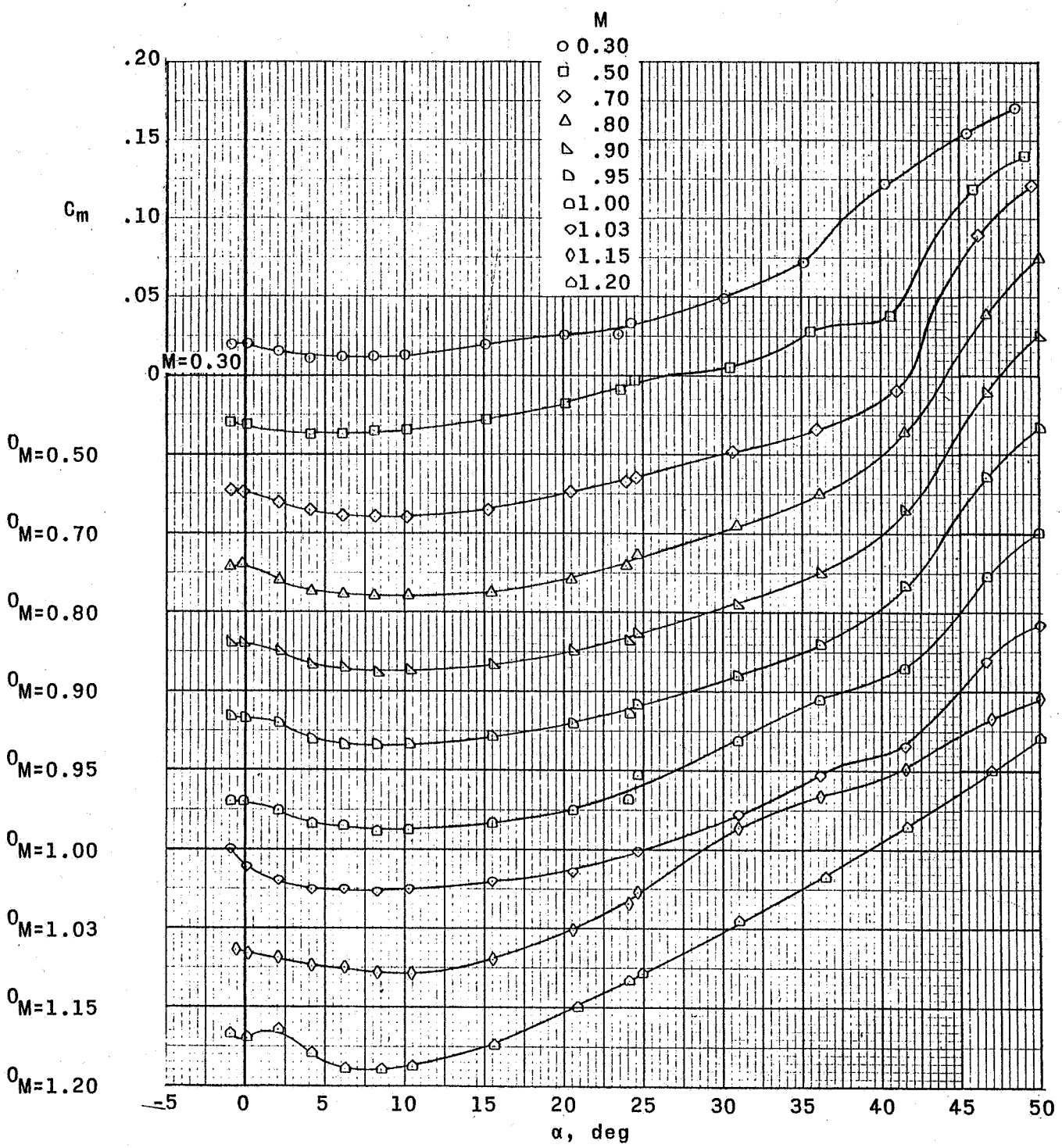

(g) Pitching-moment coefficient.
c.g. = X/D = 0.507 Z/D = 0.0444

Figure 4.- Continued. [redacted]

[redacted]

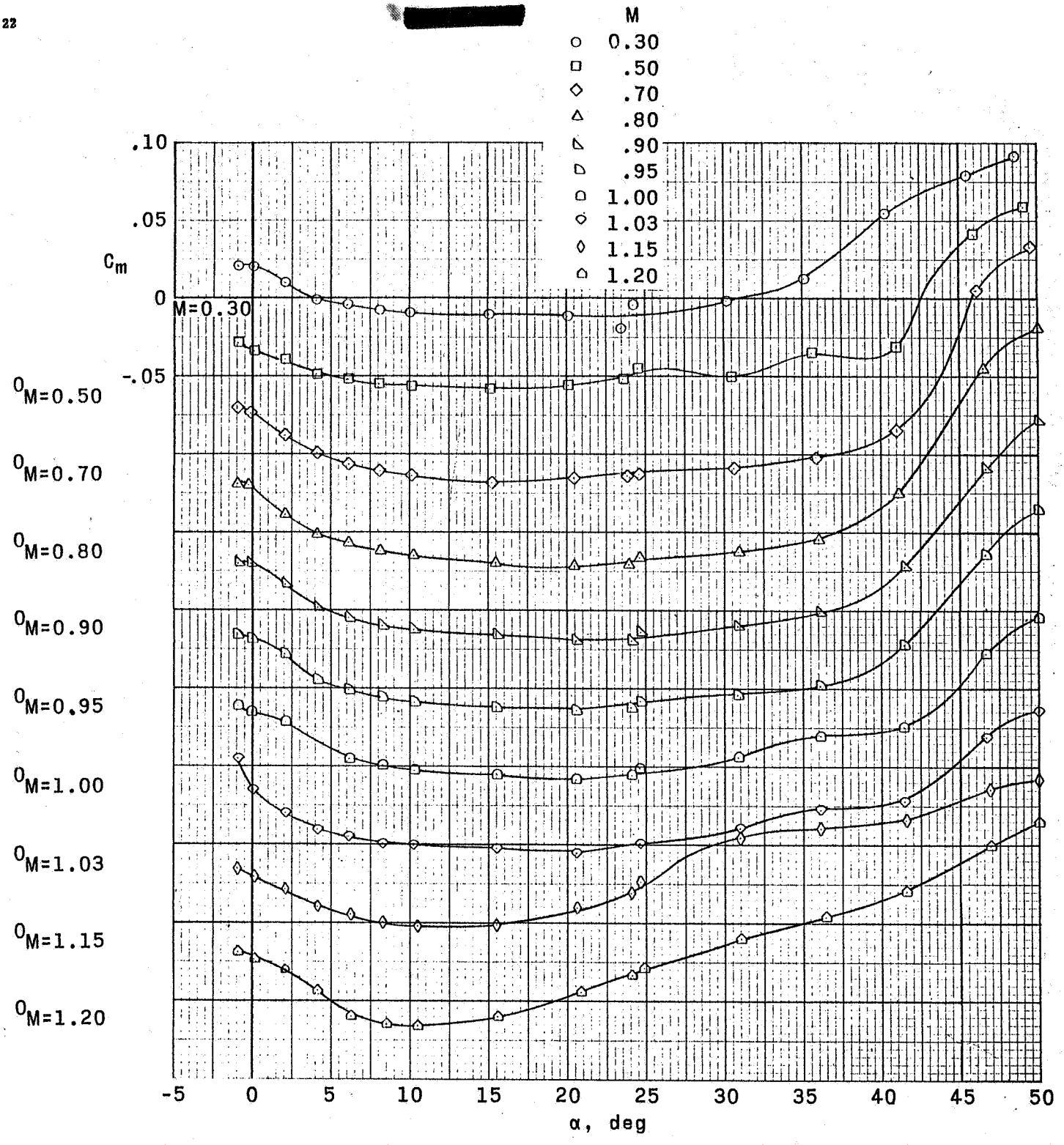

(h) Pitching-moment coefficient.
c.g. = X/D = 0.611 Z/D = 0.0427

Figure 4.- Continued. [redacted]

[redacted]

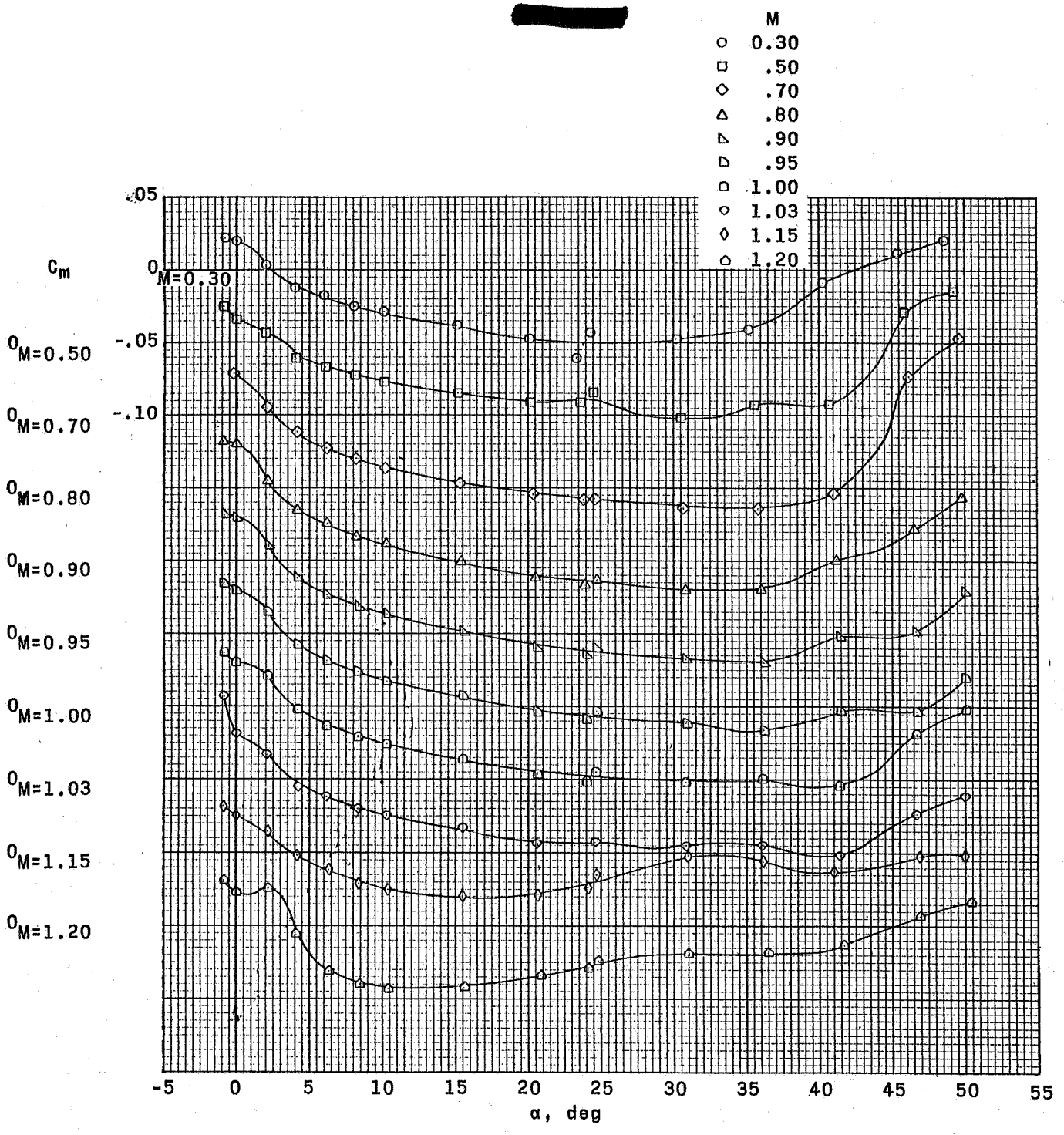

(i) Pitching-moment coefficient.
c.g. = X/D = 0.706 Z/D = 0.0407

Figure 4.- Concluded.

[redacted]

[redacted]

[redacted]

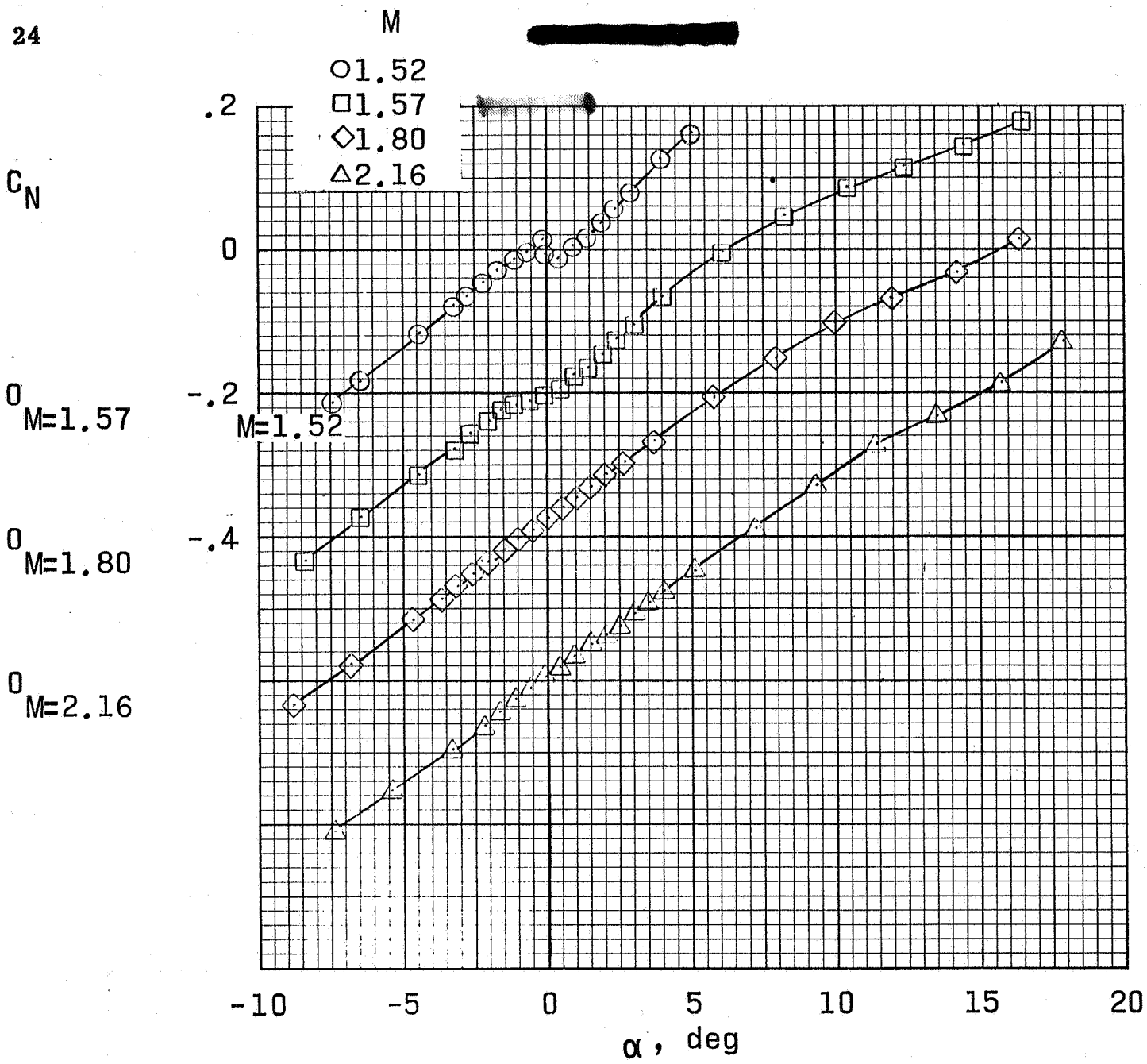

(a) Normal-force coefficient.

Figure 5.- Aerodynamic characteristics of the atmospheric abort configuration without the conical shroud around rocket nozzles at Mach numbers from 1.46 to 2.16.

[redacted]

[redacted]

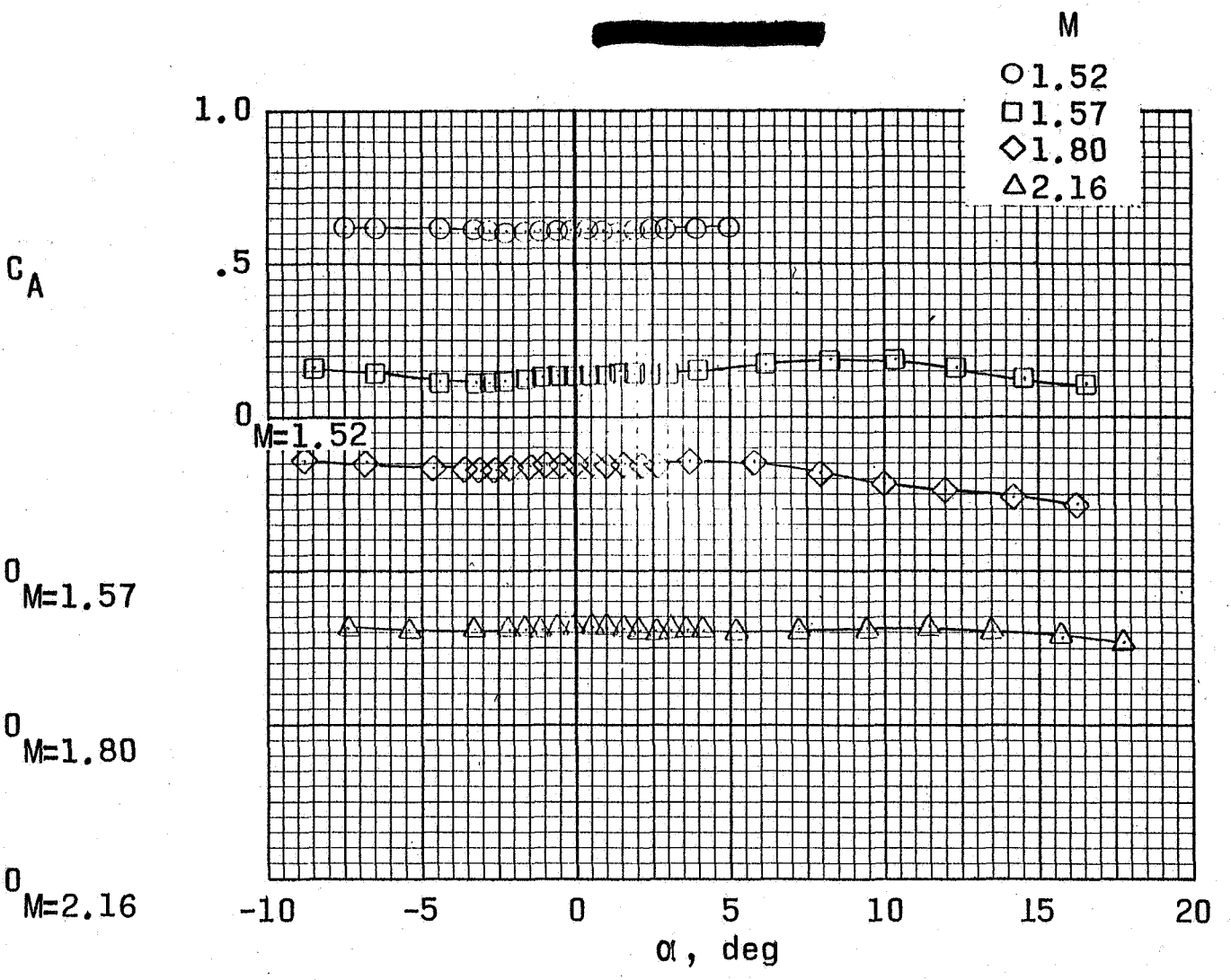

(b) Axial-force coefficient.

Figure 5.- Continued.

[redacted]

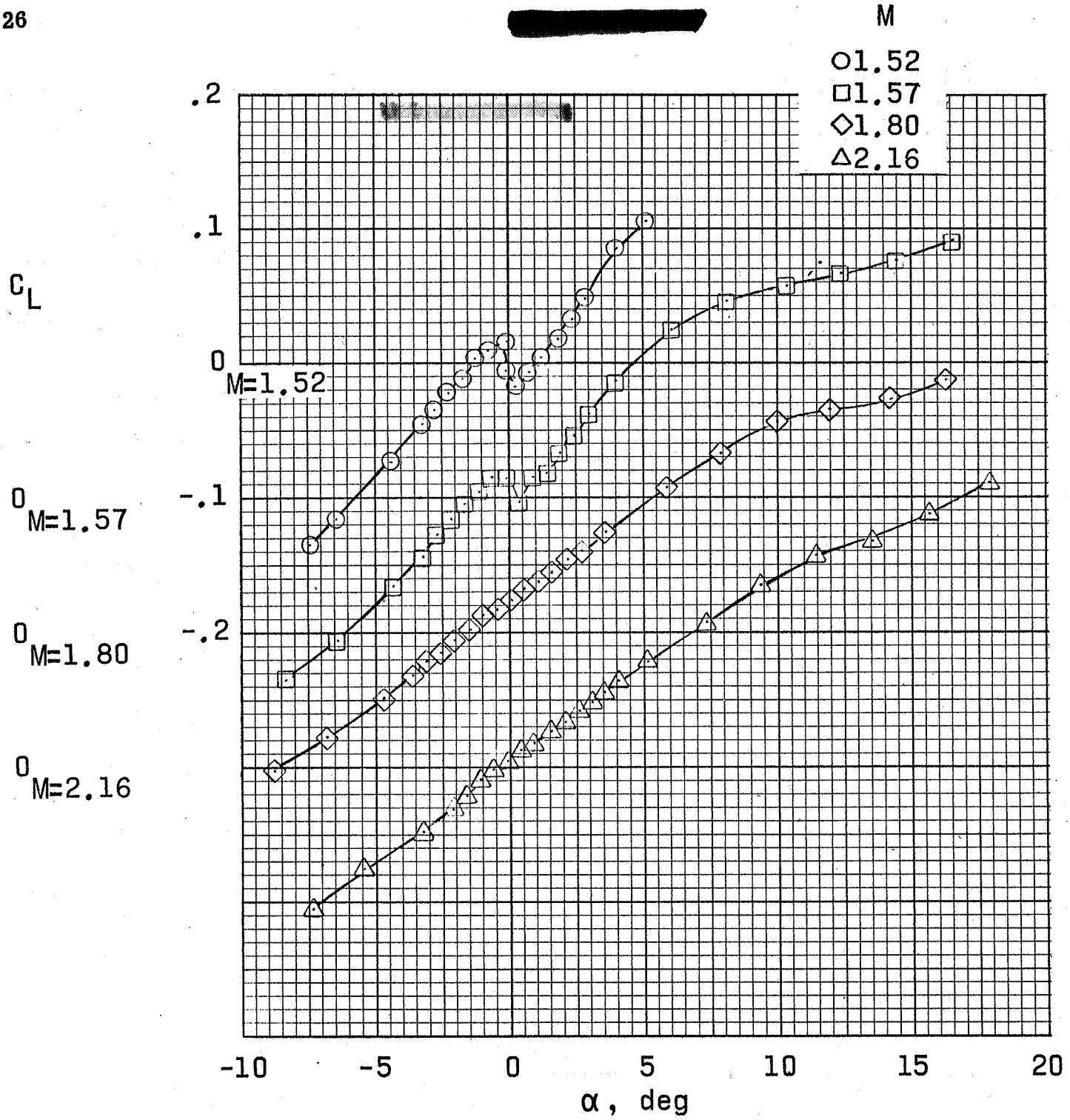

(c) Lift coefficient.

Figure 5.- Continued.

[redacted]

[redacted]

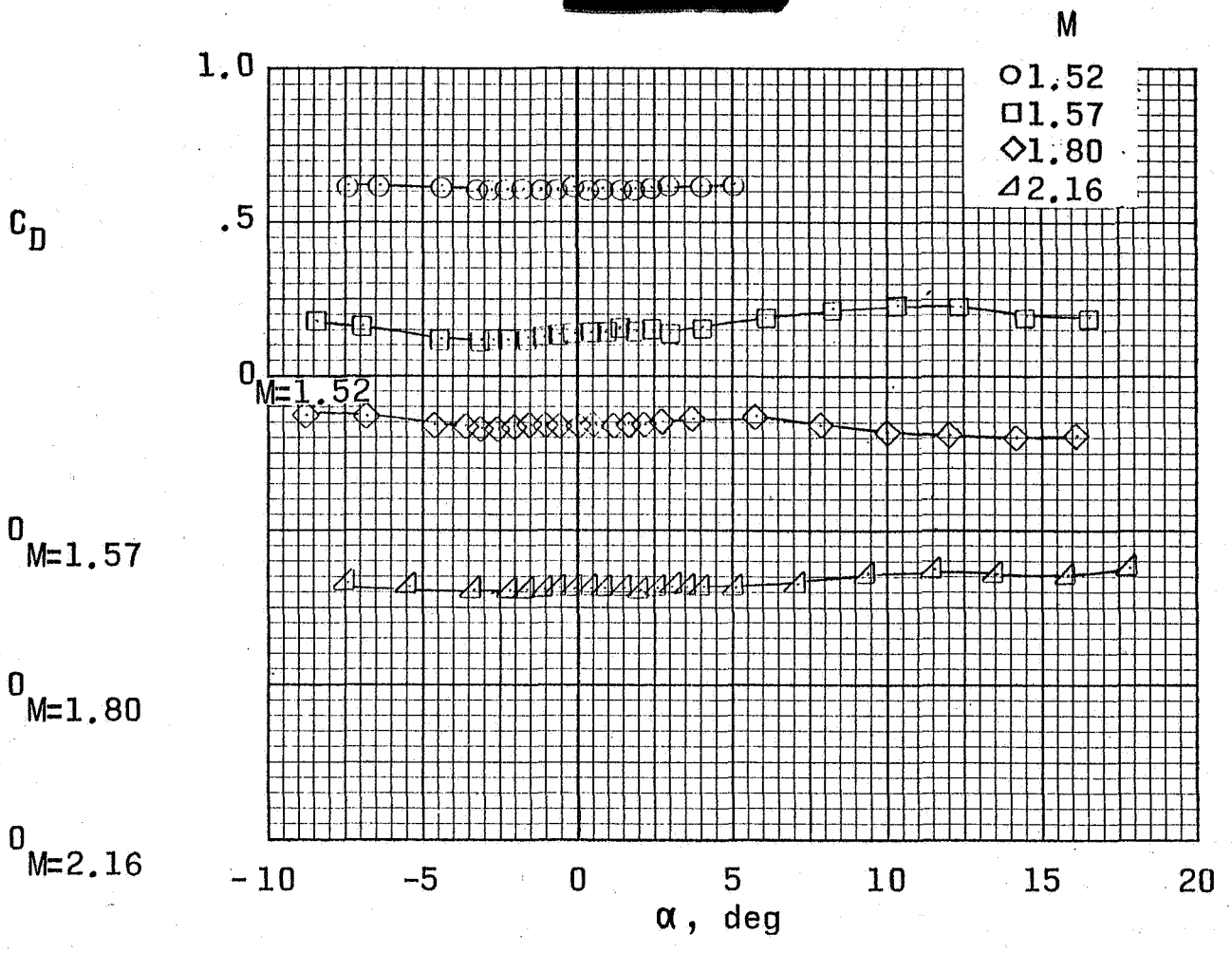

(d) Drag coefficient.

Figure 5.- Continued.

[redacted]

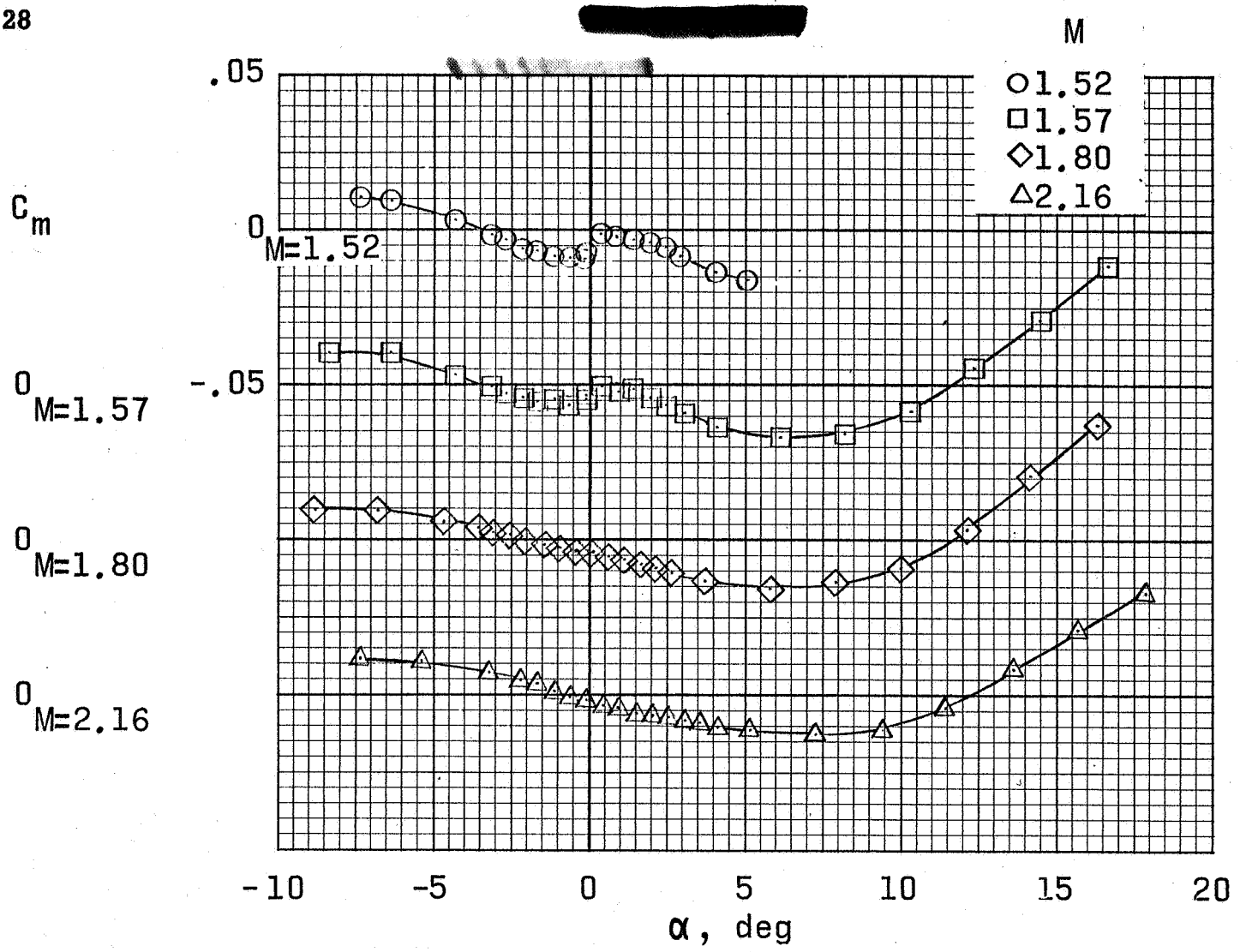

(e) Pitching-moment coefficient.
c.g. = X/D = 0.390 Z/D = 0.000

Figure 5.- Continued.

[redacted]

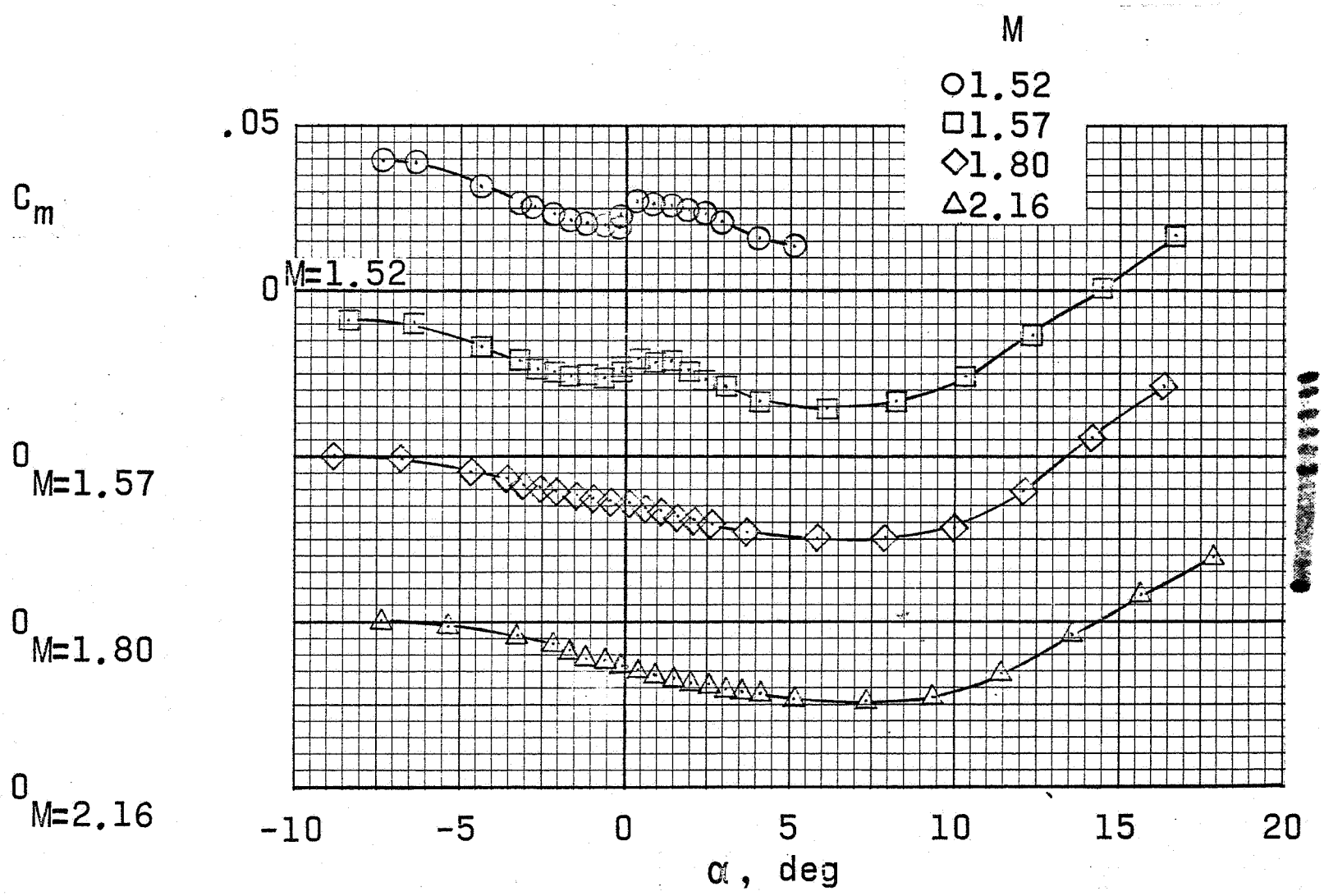

(f) Pitching-moment coefficient.
c.g. = X/D = 0.390 Z/D = 0.0473

Figure 5.- Continued.

[redacted]

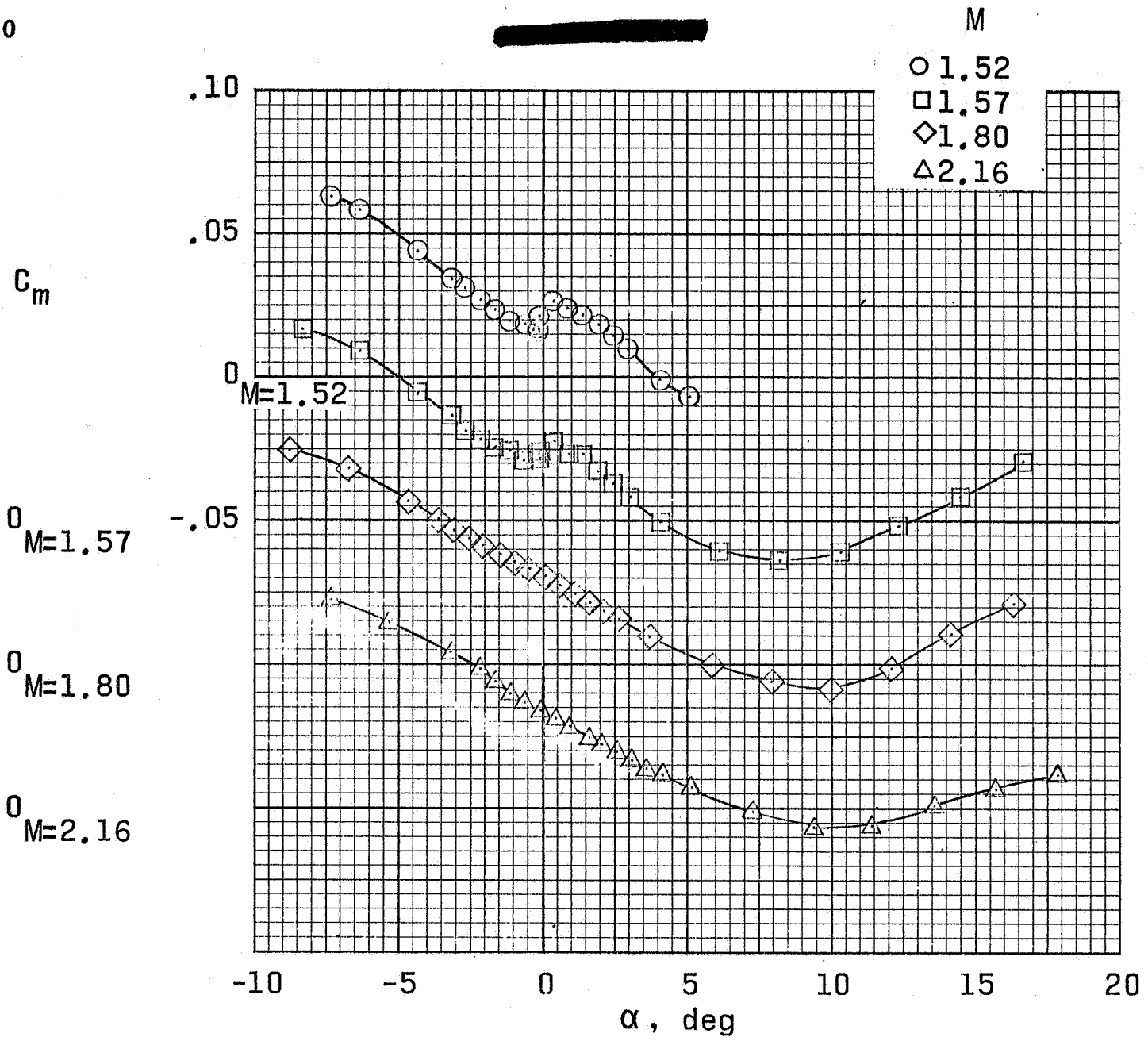

(g) Pitching-moment coefficient.
c.g. = X/D = 0.507 Z/D = 0.0444

Figure 5.- Continued.

[redacted]

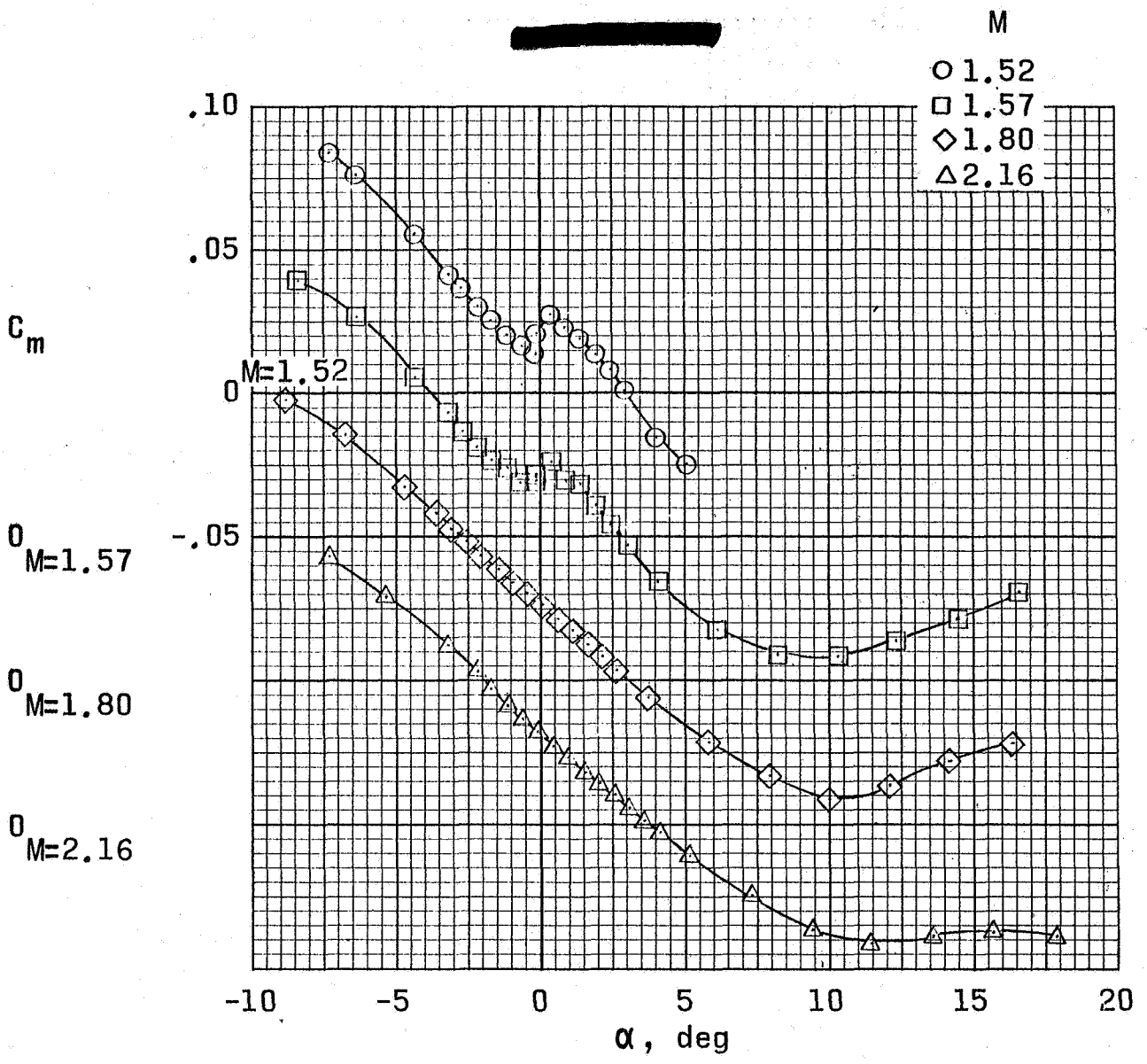

(h) Pitching=moment coefficient.
c.g. = X/D = 0.611 Z/D = 0.0427

Figure 5.- Continued.

[redacted]

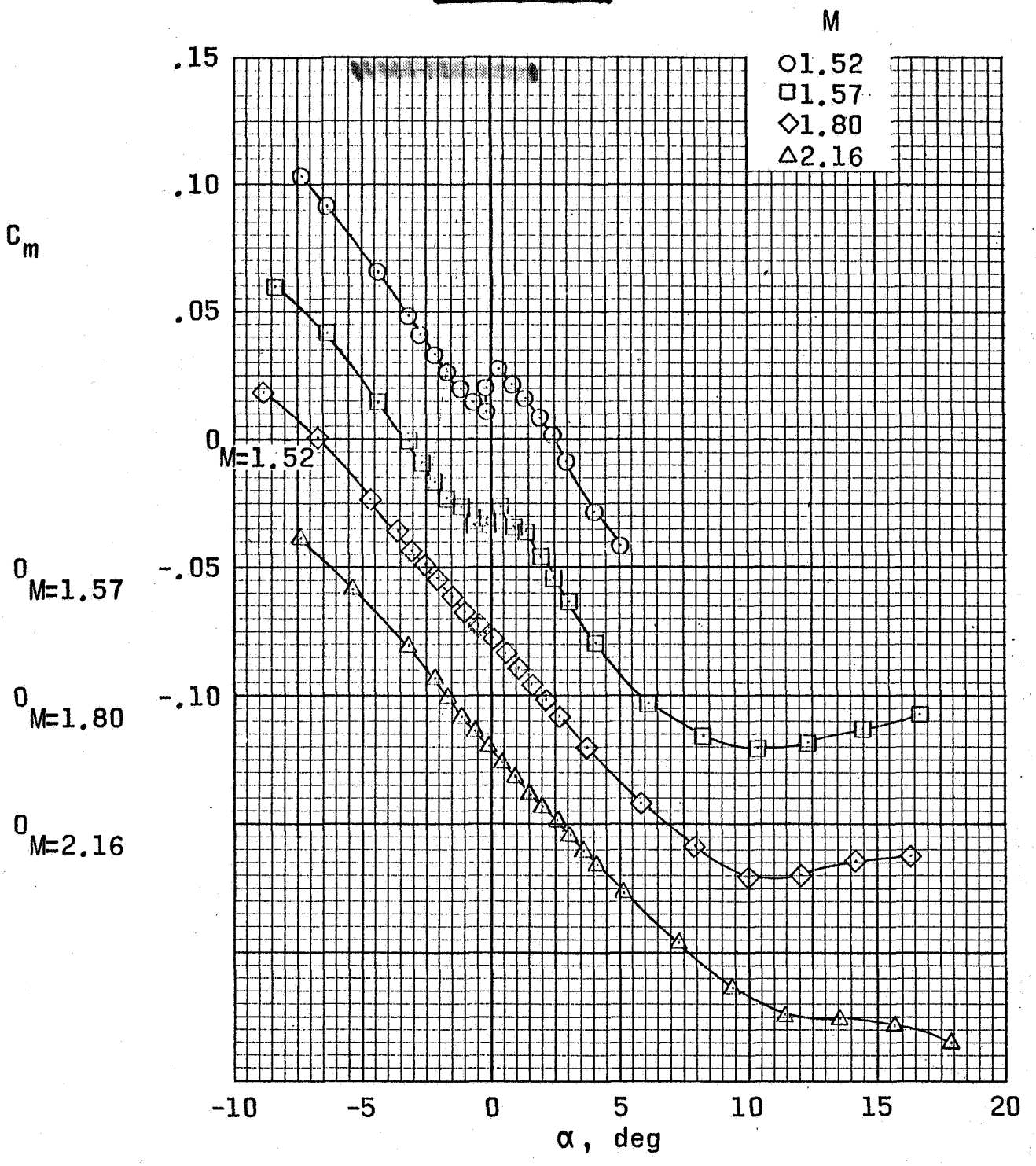

(i) Pitching-moment coefficient.
c.g. = X/D = 0.706 Z/D = 0.0407

Figure 5.- Concluded.

[redacted]

[redacted]

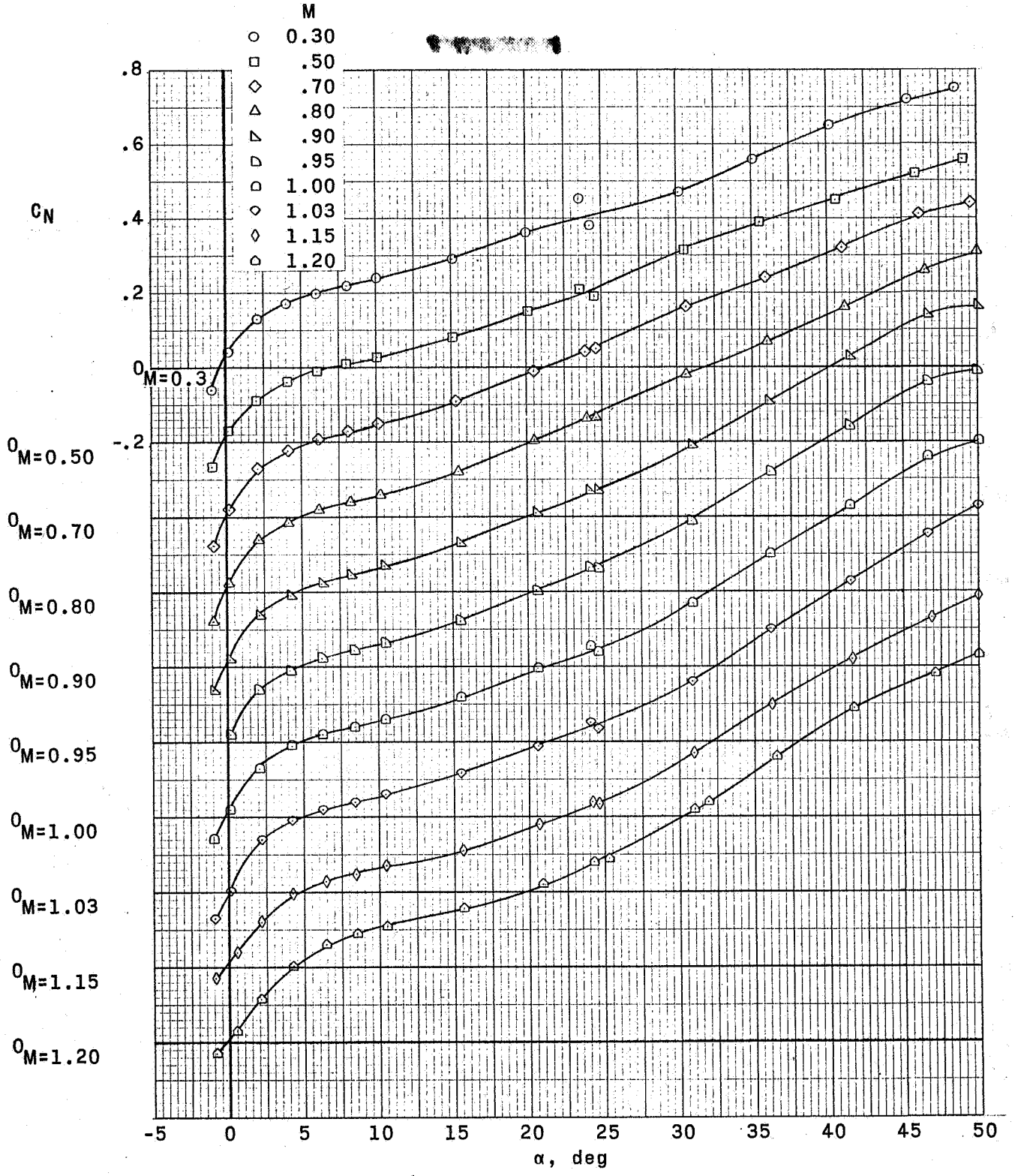

(a) Normal-force coefficient.

Figure 6.- Aerodynamic characteristics of the atmospheric abort configuration with the conical shroud around rocket nozzles at Mach numbers from 0.3 to 1.20.

[redacted]

[redacted]

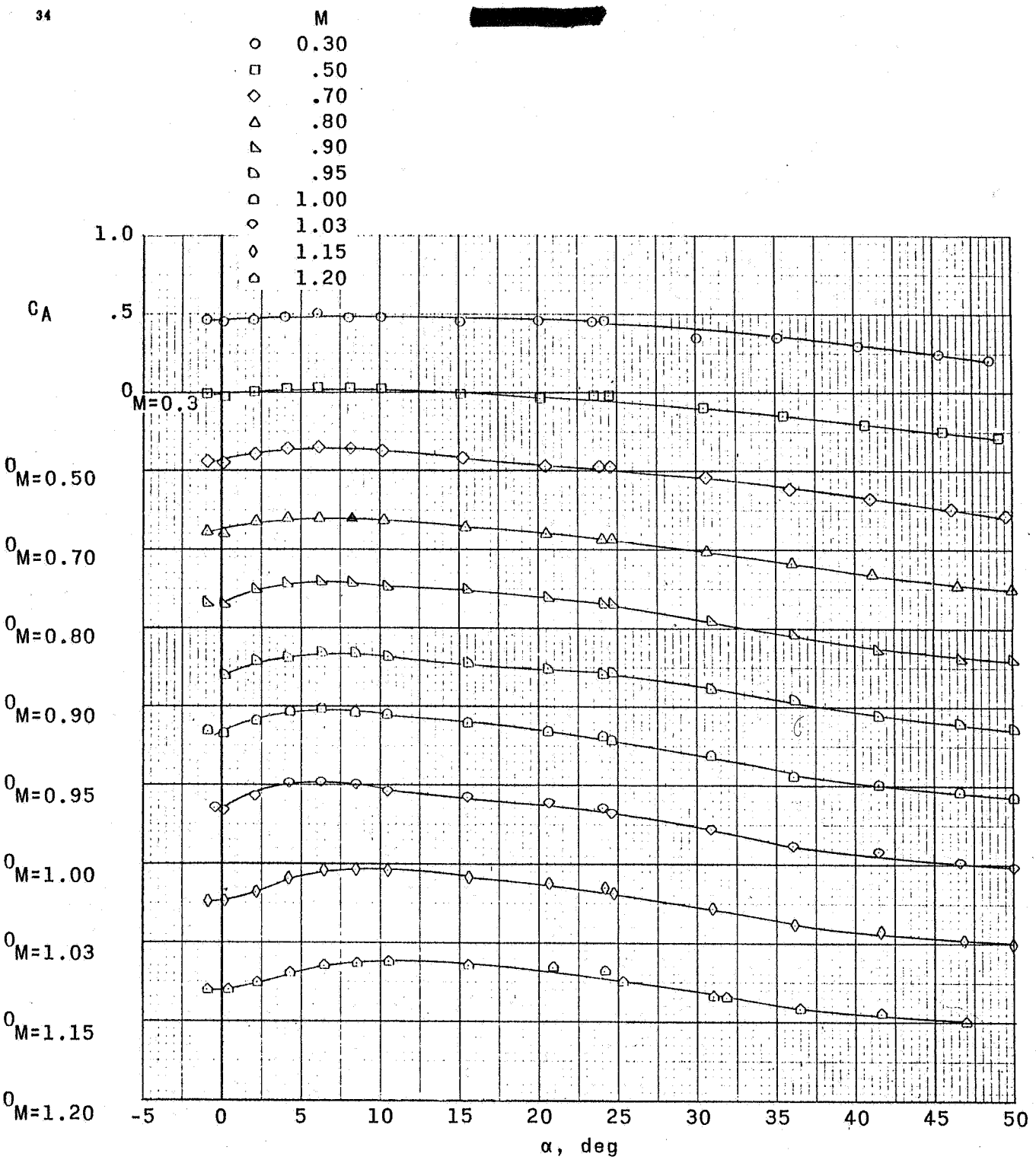

(b) Axial-force coefficient.

Figure 6.- Continued.

[redacted]

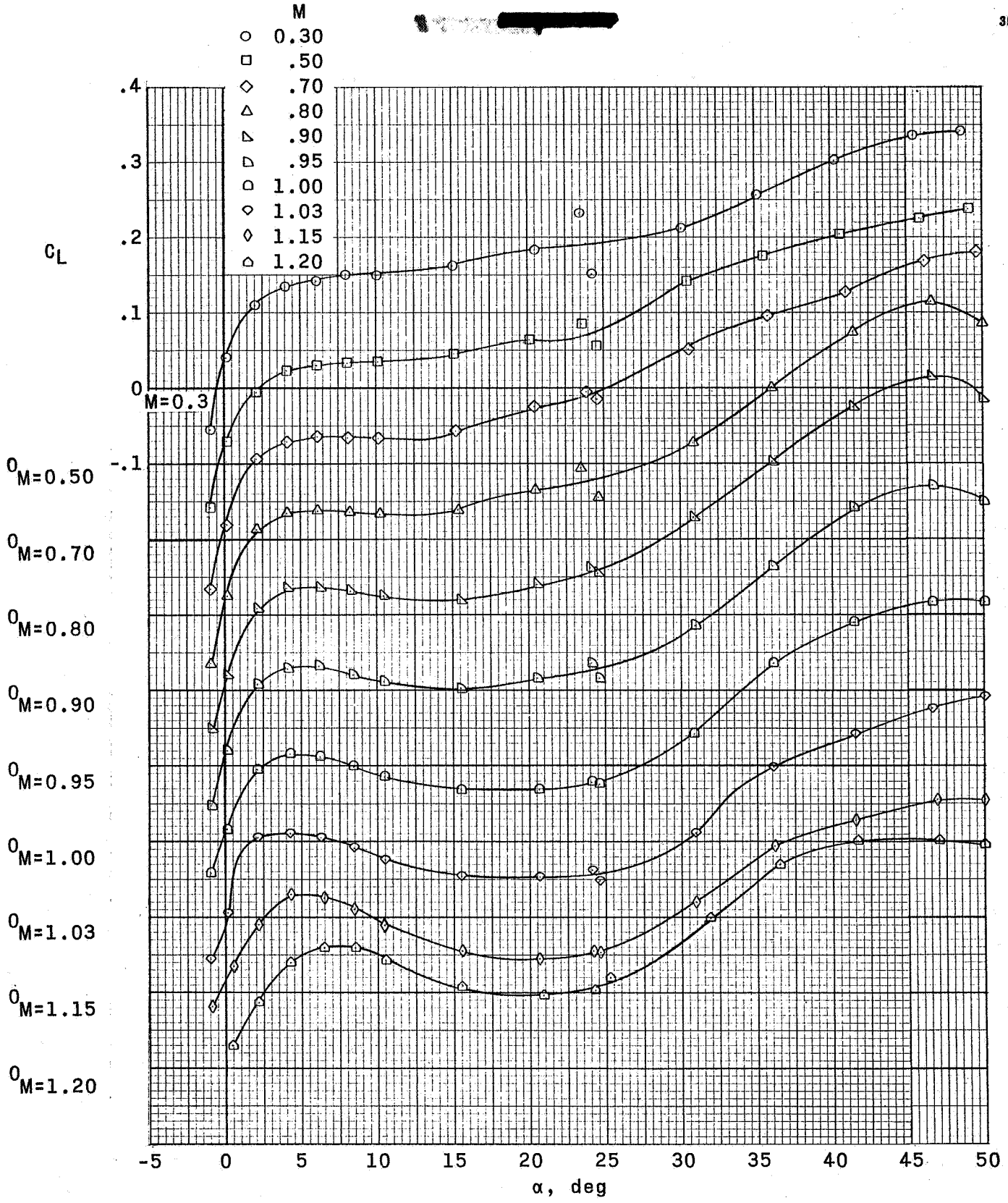

(c) Lift coefficient.

Figure 6.- Continued. [redacted]

[redacted]

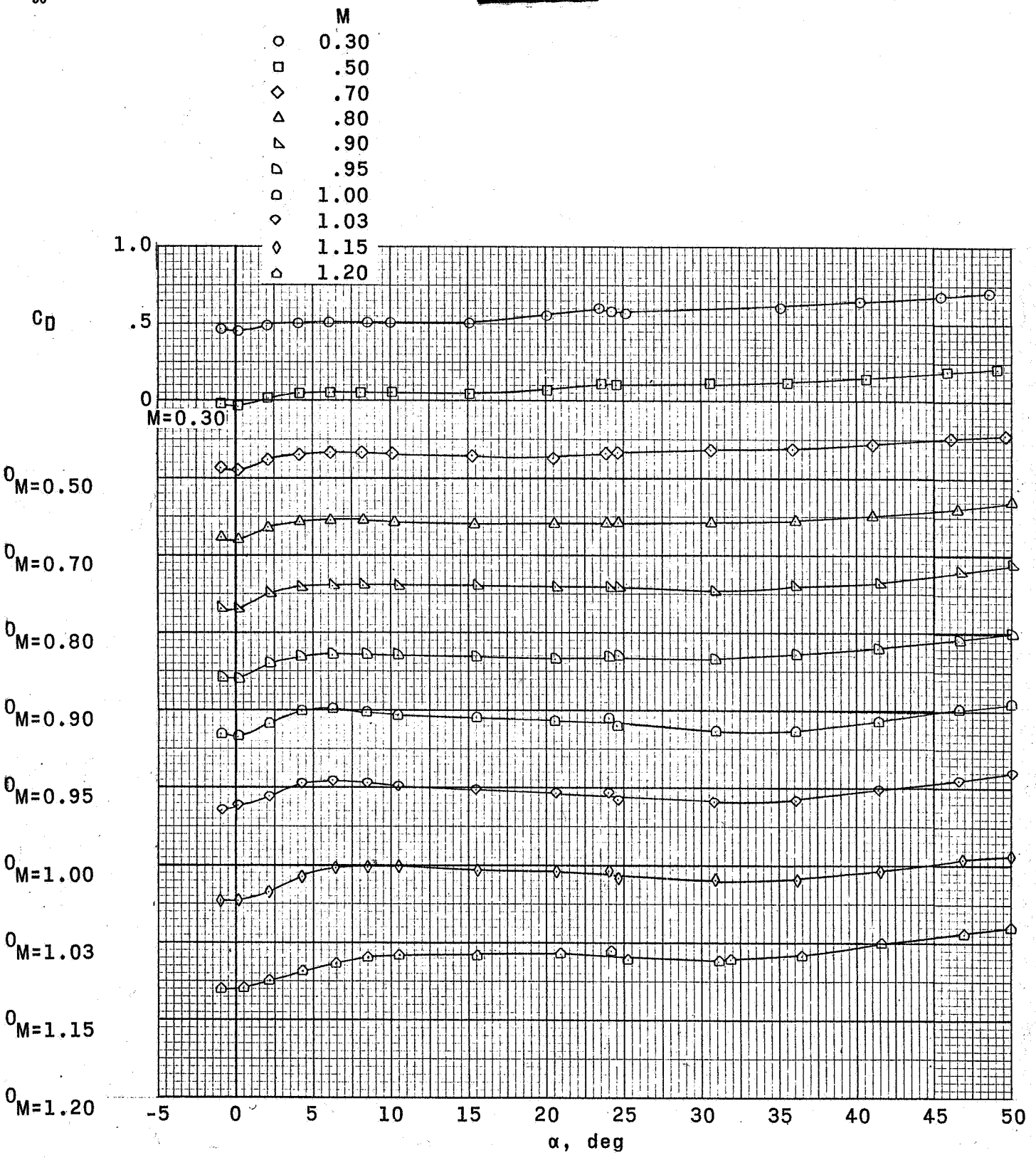

(d) Drag coefficient.

Figure 6.- Continued. [redacted]

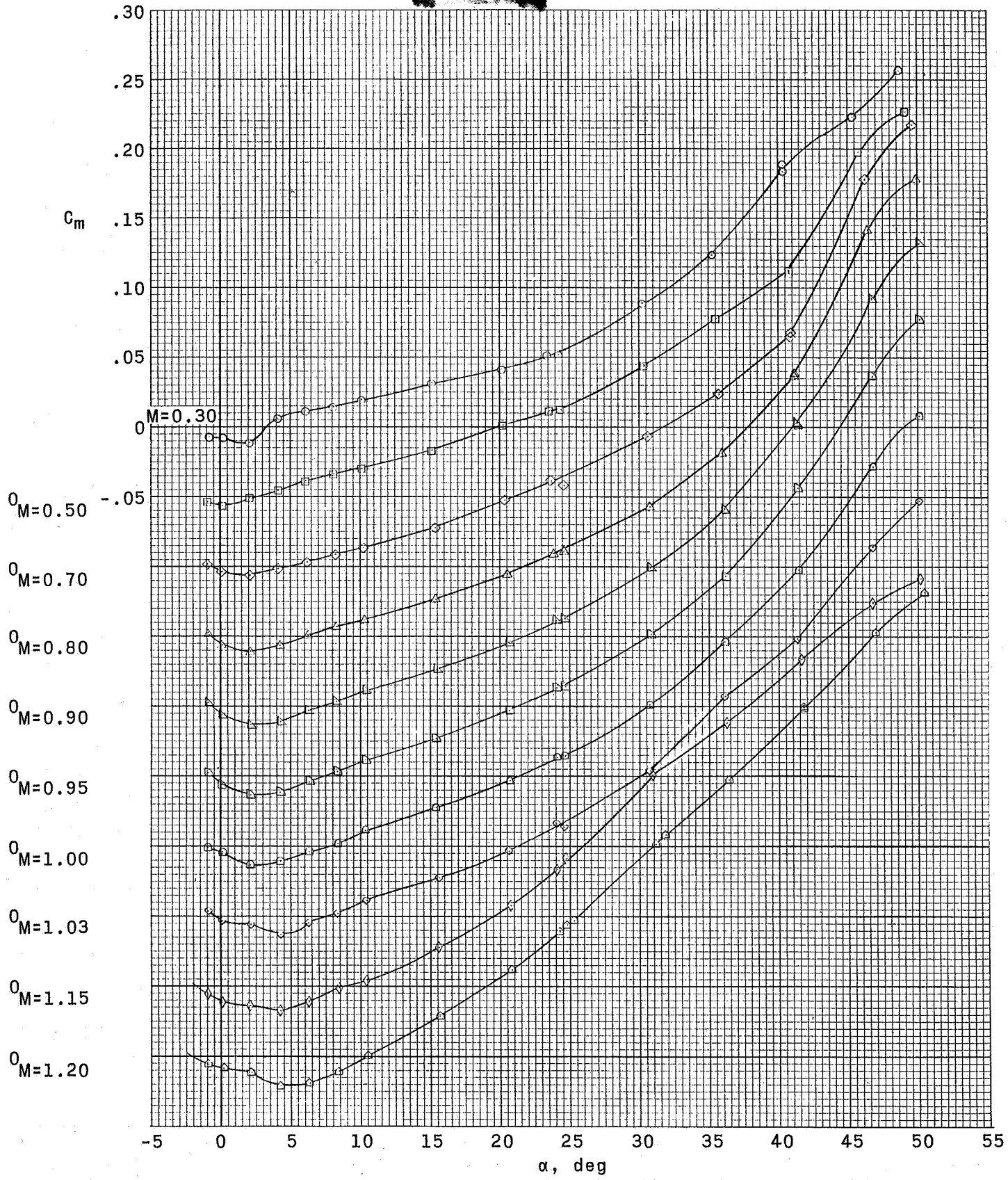

(e) Pitching-moment coefficient.
c.g. = X/D = 0.390 Z/D = 0.000

Figure 6.- Continued. [redacted]

[redacted]

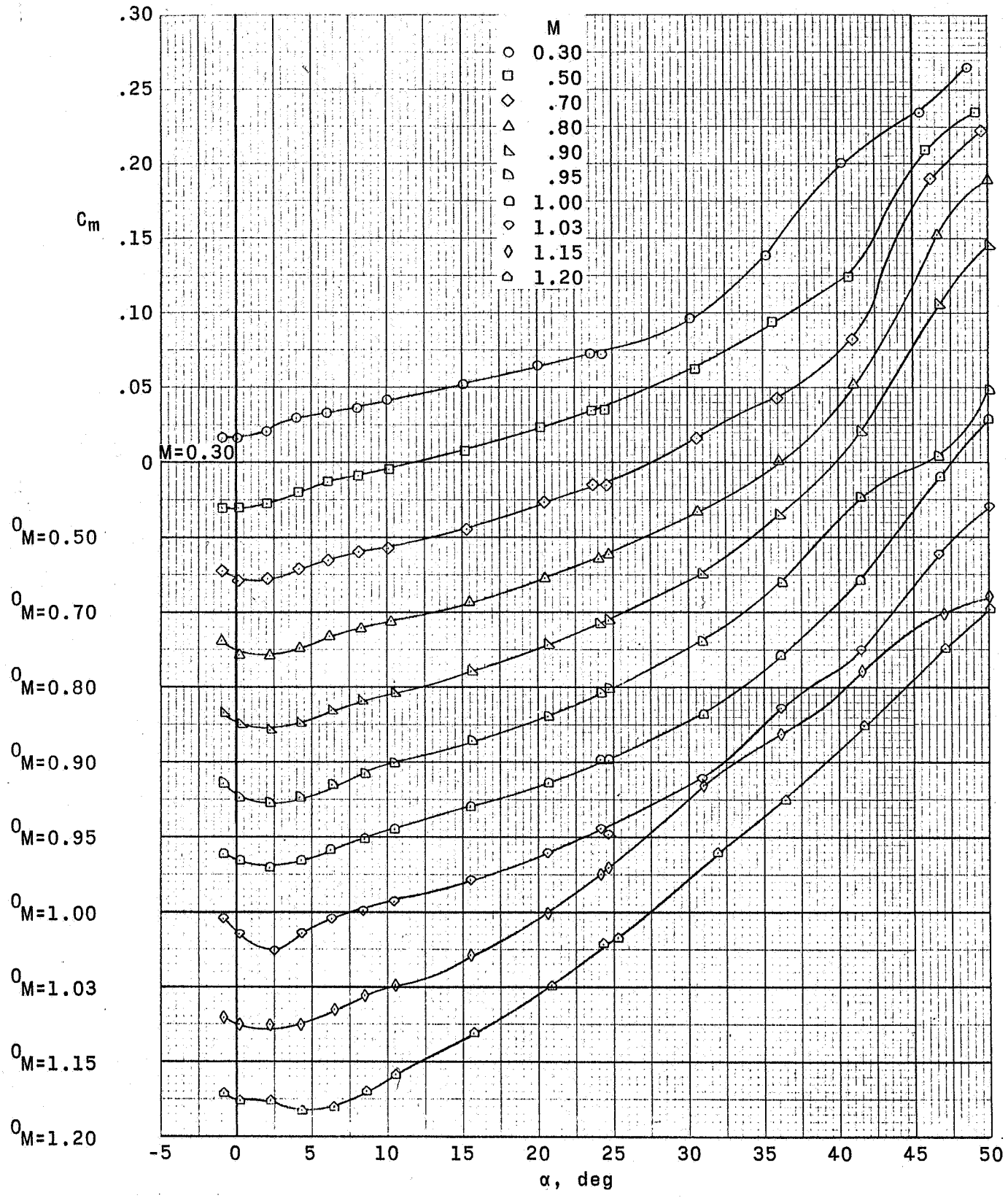

(f) Pitching-moment coefficient.
c.g. = X/D = 0.390 Z/D = 0.0473

Figure 6.- Continued.

[redacted]

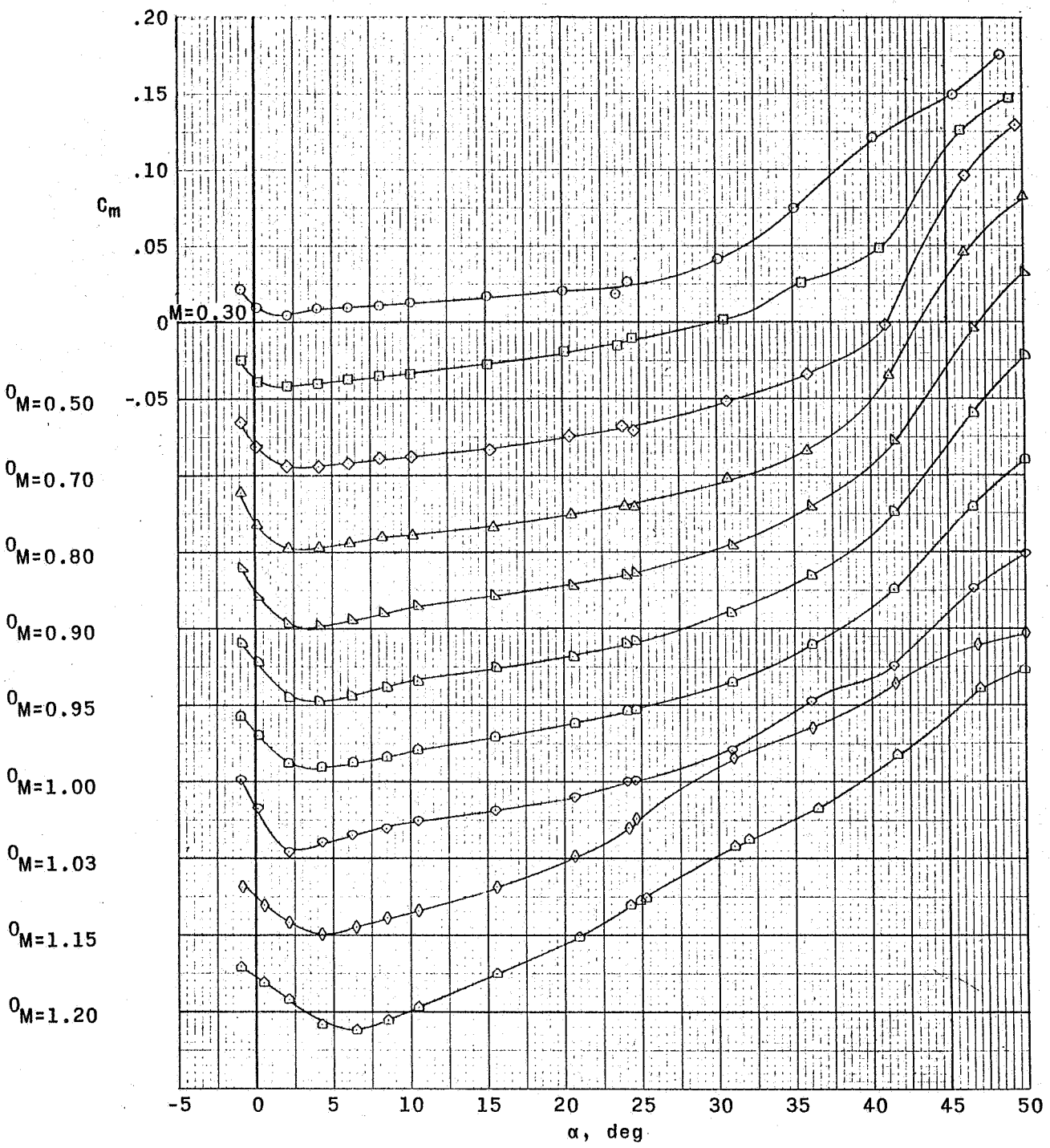

(g) Pitching-moment coefficient.
c.g. = X/D = 0.507 Z/D = 0.0444

Figure 6.- Continued.

[redacted]

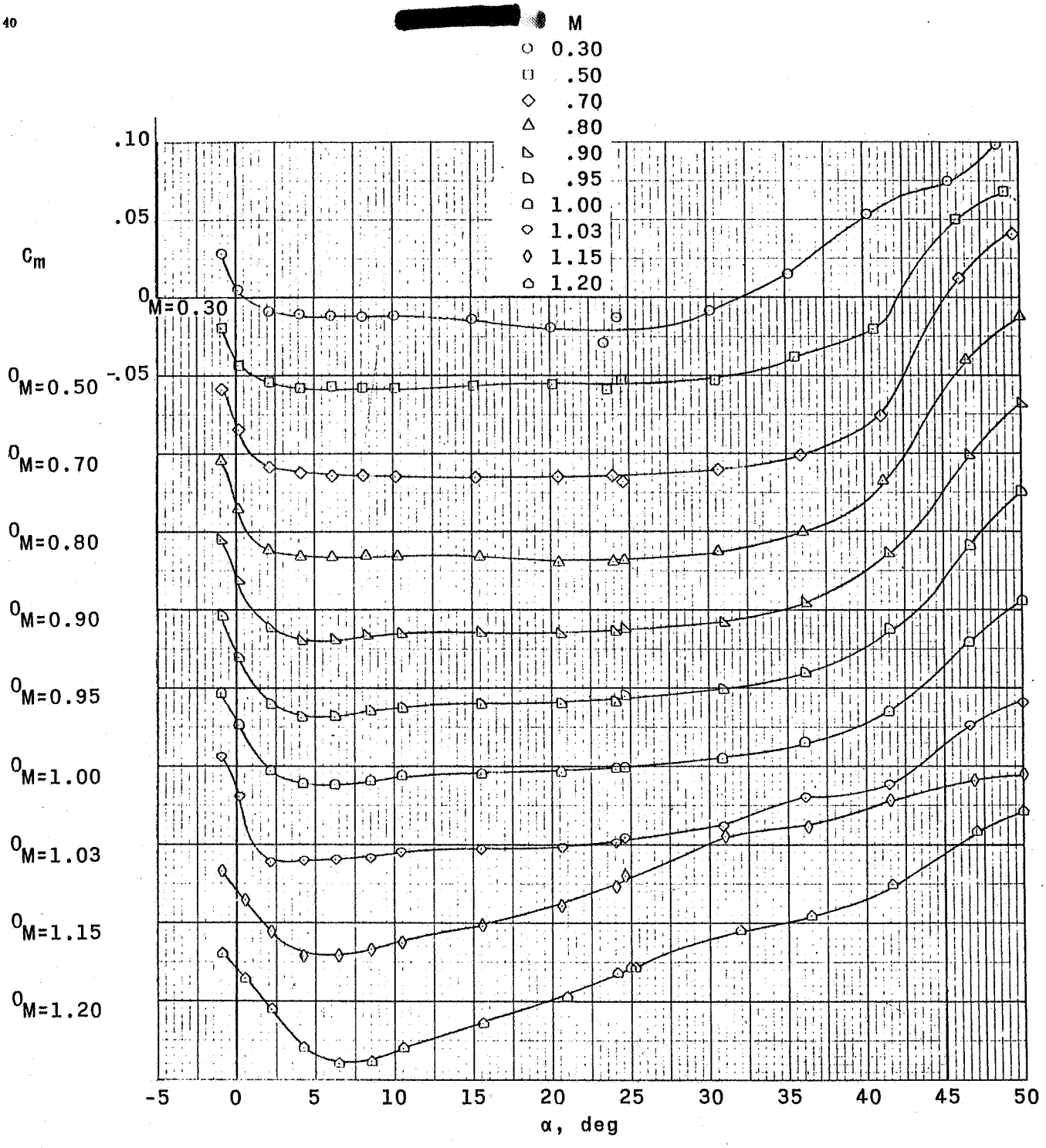

(h) Pitching-moment coefficient.
c.g. = X/D = 0.611 Z/D = 0.0427

Figure 6.- Continued.

[redacted]

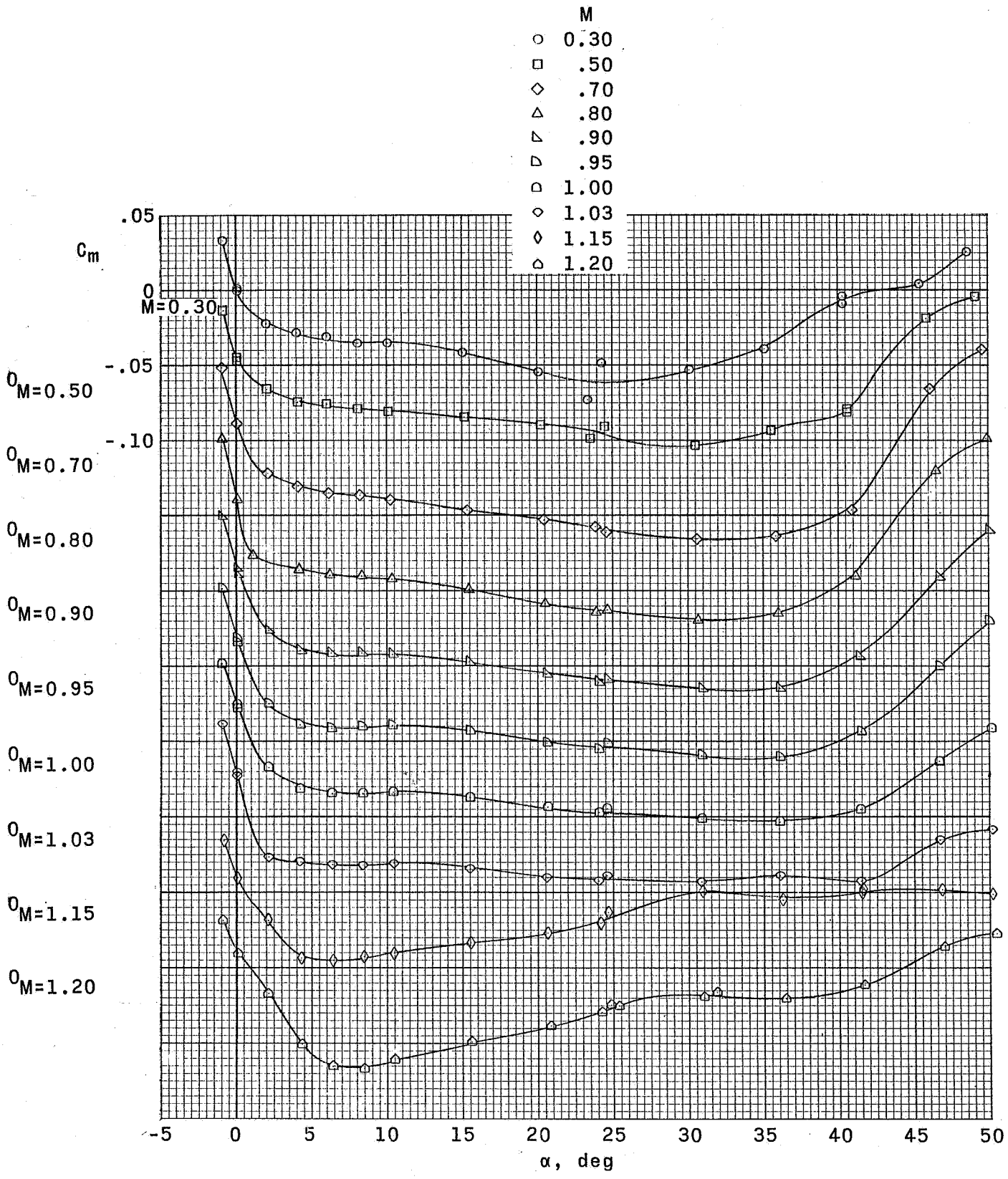

(i) Pitching-moment coefficient.
c.g. = X/D = 0.706 Z/D = 0.0407

Figure 6.- Concluded.

[redacted]

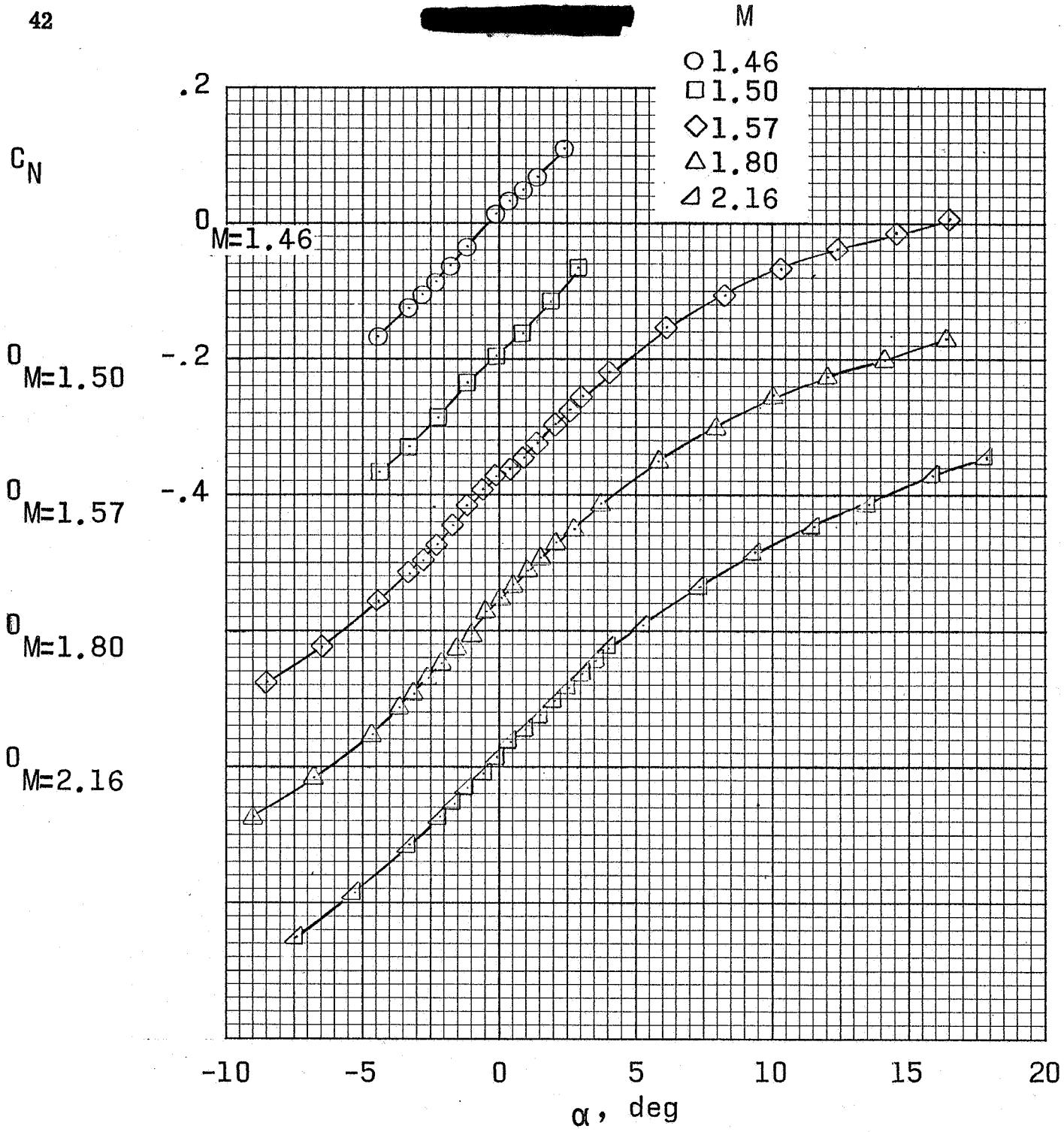

(a) Normal-force coefficient.

Figure 7.- Aerodynamic characteristics of the atmospheric abort configuration with the conical shroud around rocket nozzles at Mach numbers from 1.46 to 2.16.

[redacted]

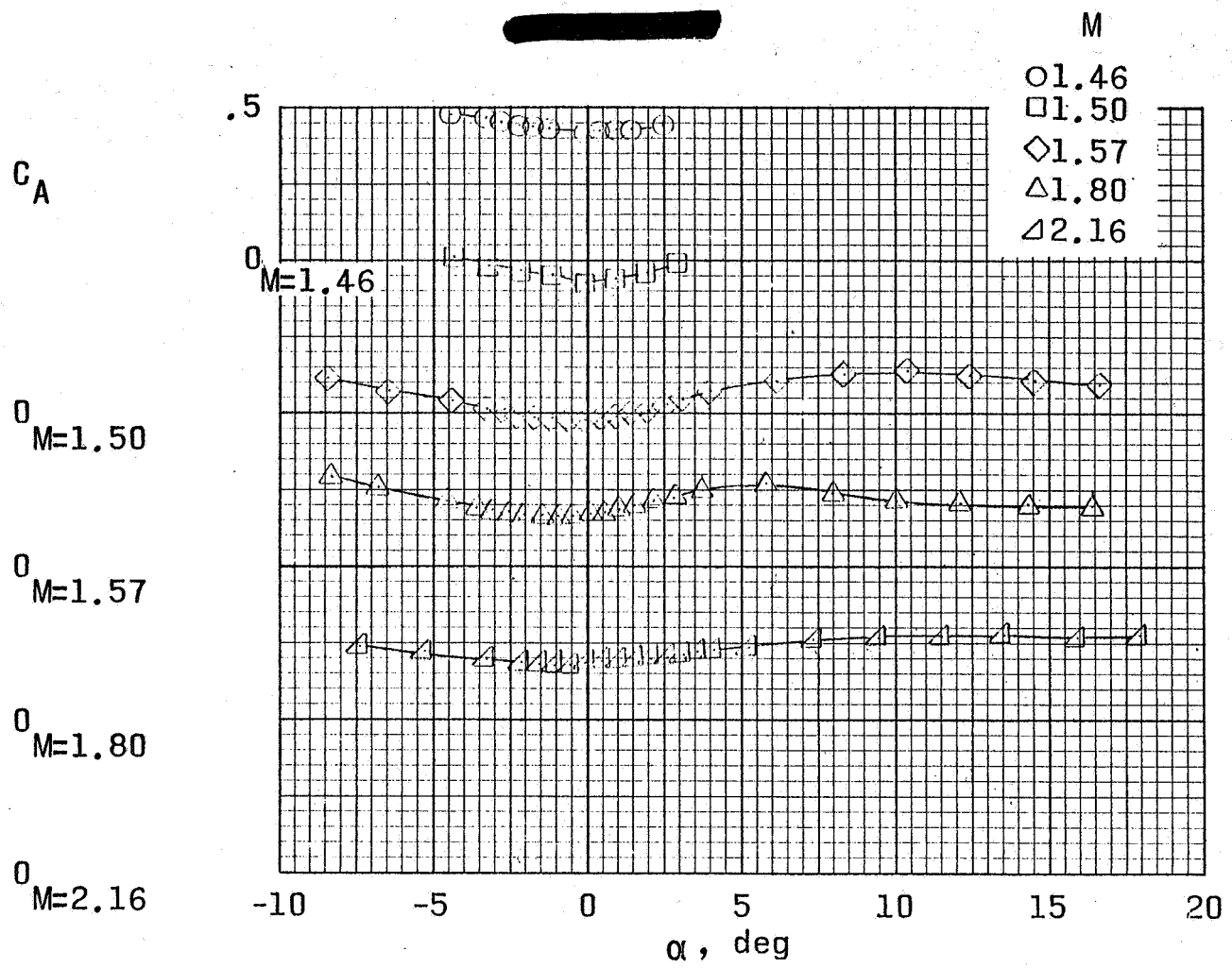

(b) Axial-force coefficient.

Figure 7.- Continued.

[redacted]

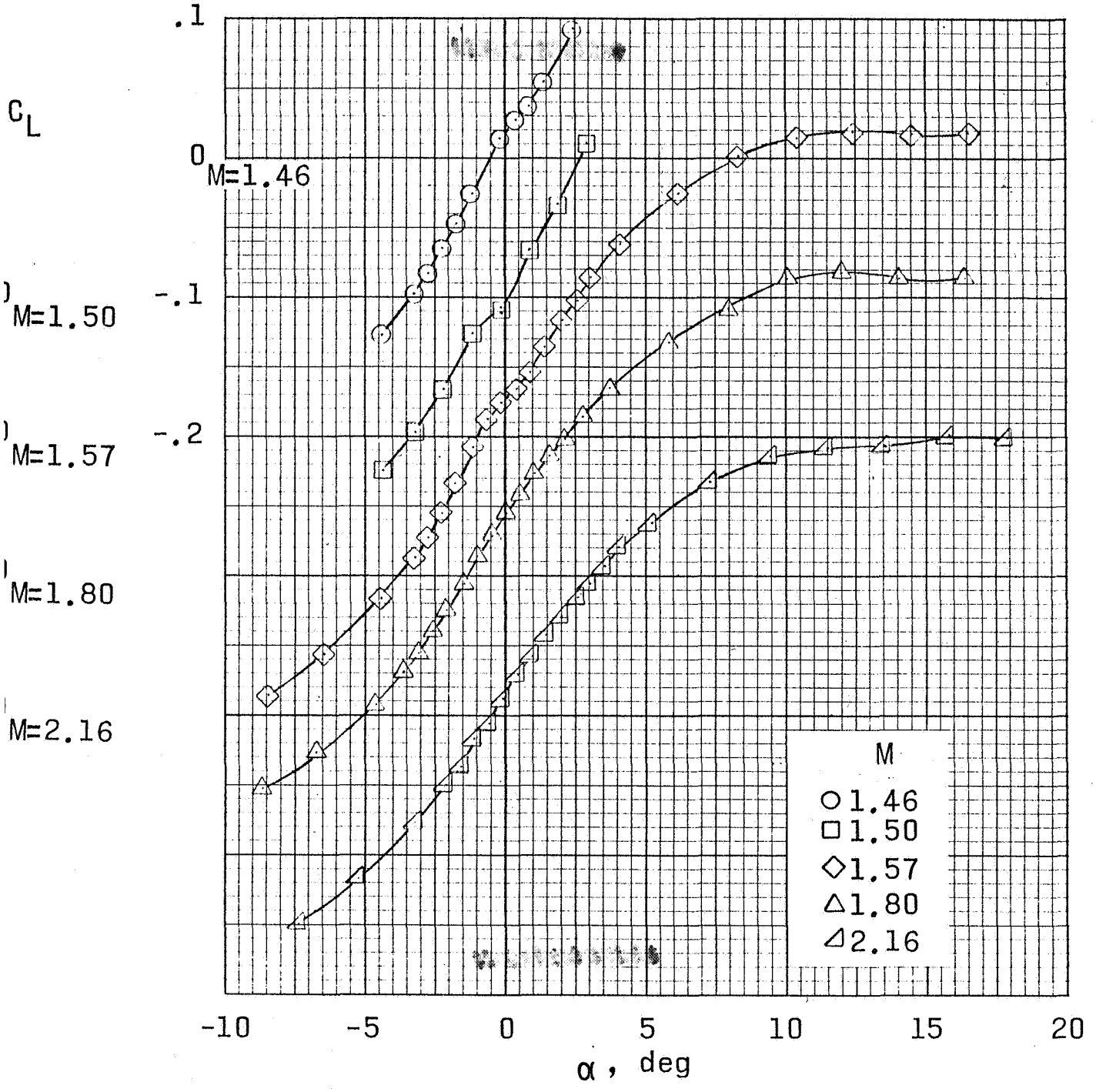

(c) Lift coefficient.

Figure 7.- Continued.

[redacted]

[redacted]

[redacted]

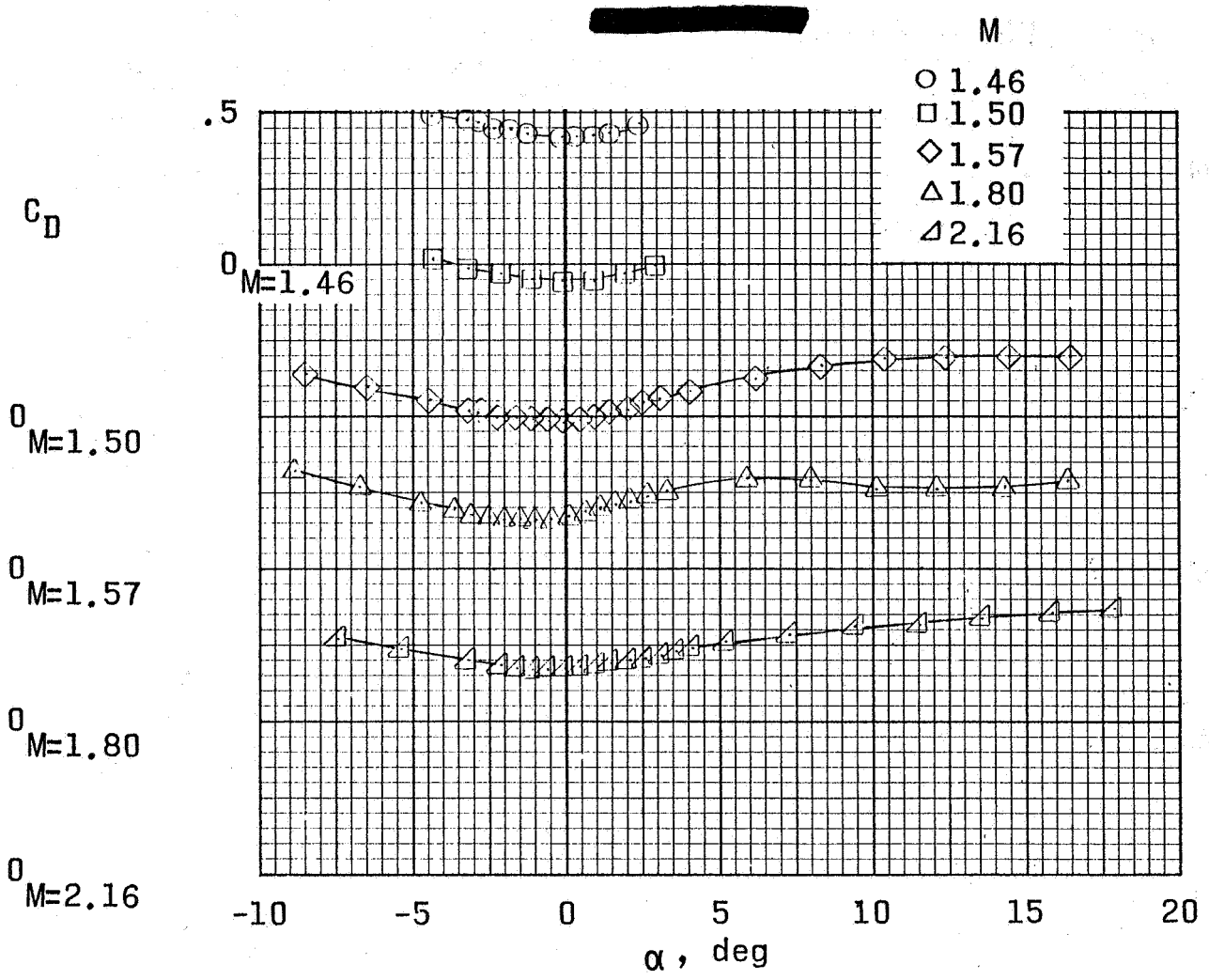

(d) Drag coefficient.

Figure 7.- Continued.

[redacted]

[redacted]

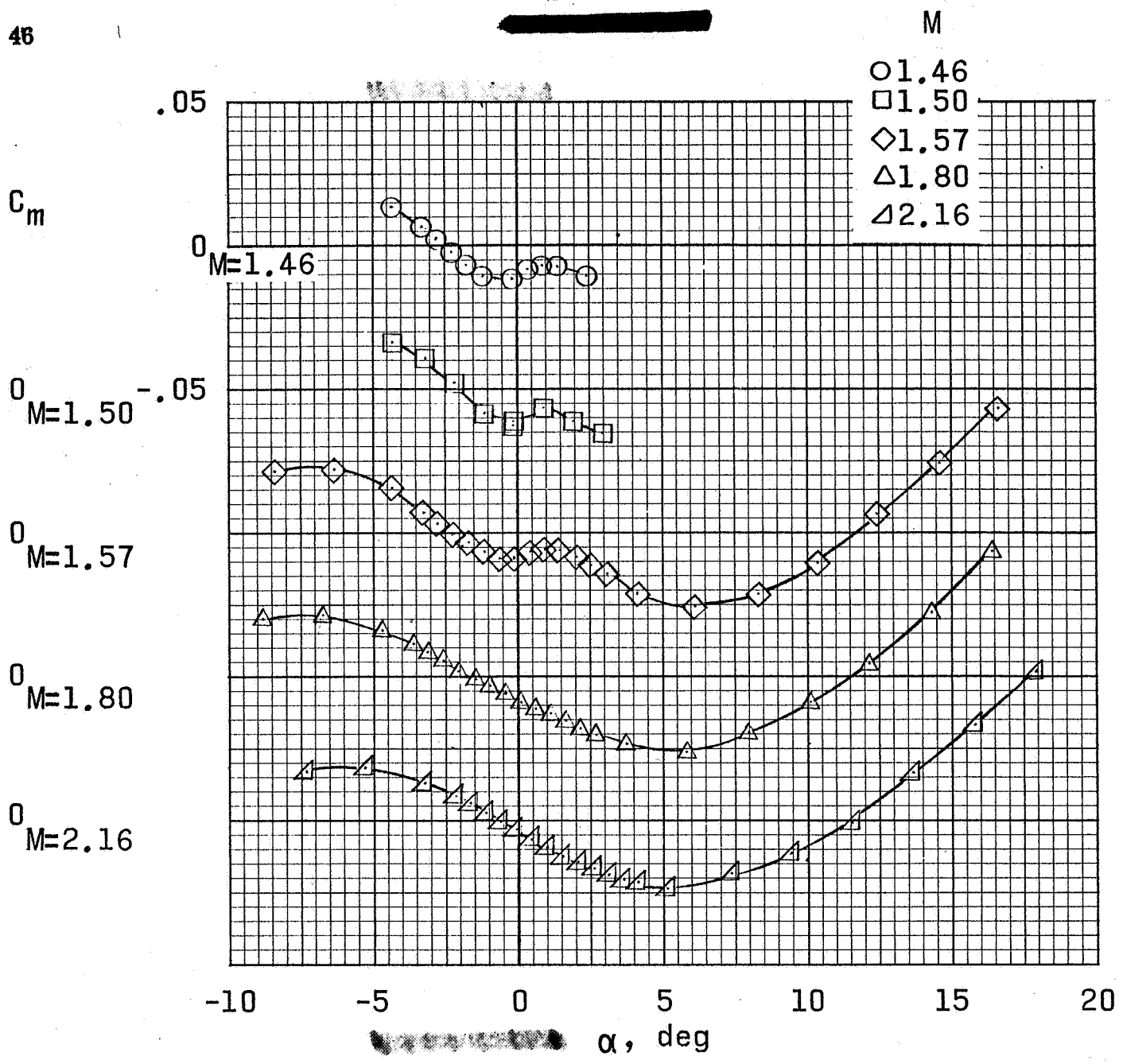

(e) Pitching-moment coefficient.
c.g. = X/D = 0.390 Z/D = 0.000

Figure 7.- Continued.

[redacted]

[redacted]

[redacted]

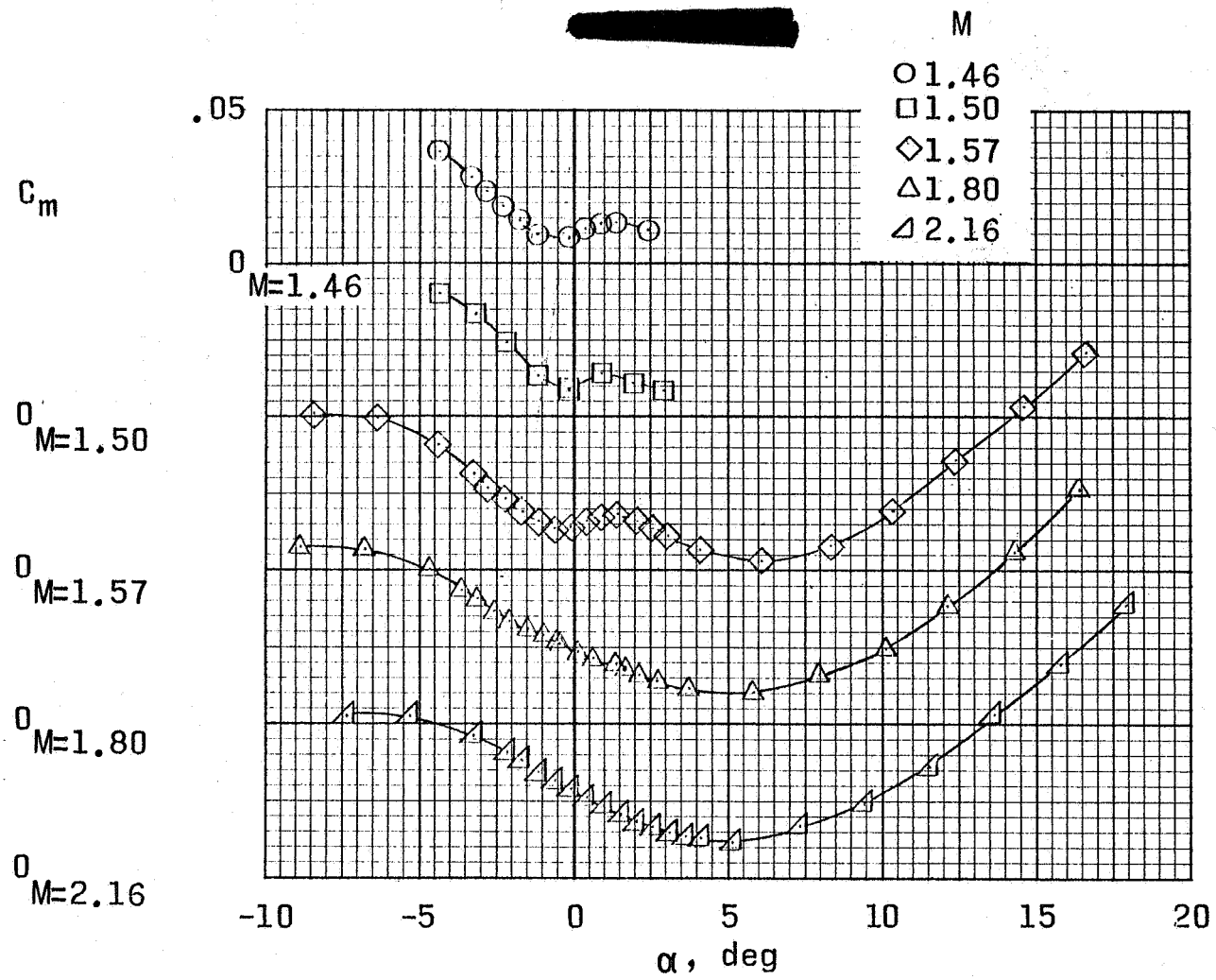

(f) Pitching-moment coefficient.
c.g. = X/D = 0.390 Z/D = 0.0473

Figure 7.- Continued.

[redacted]

[redacted]

[redacted]

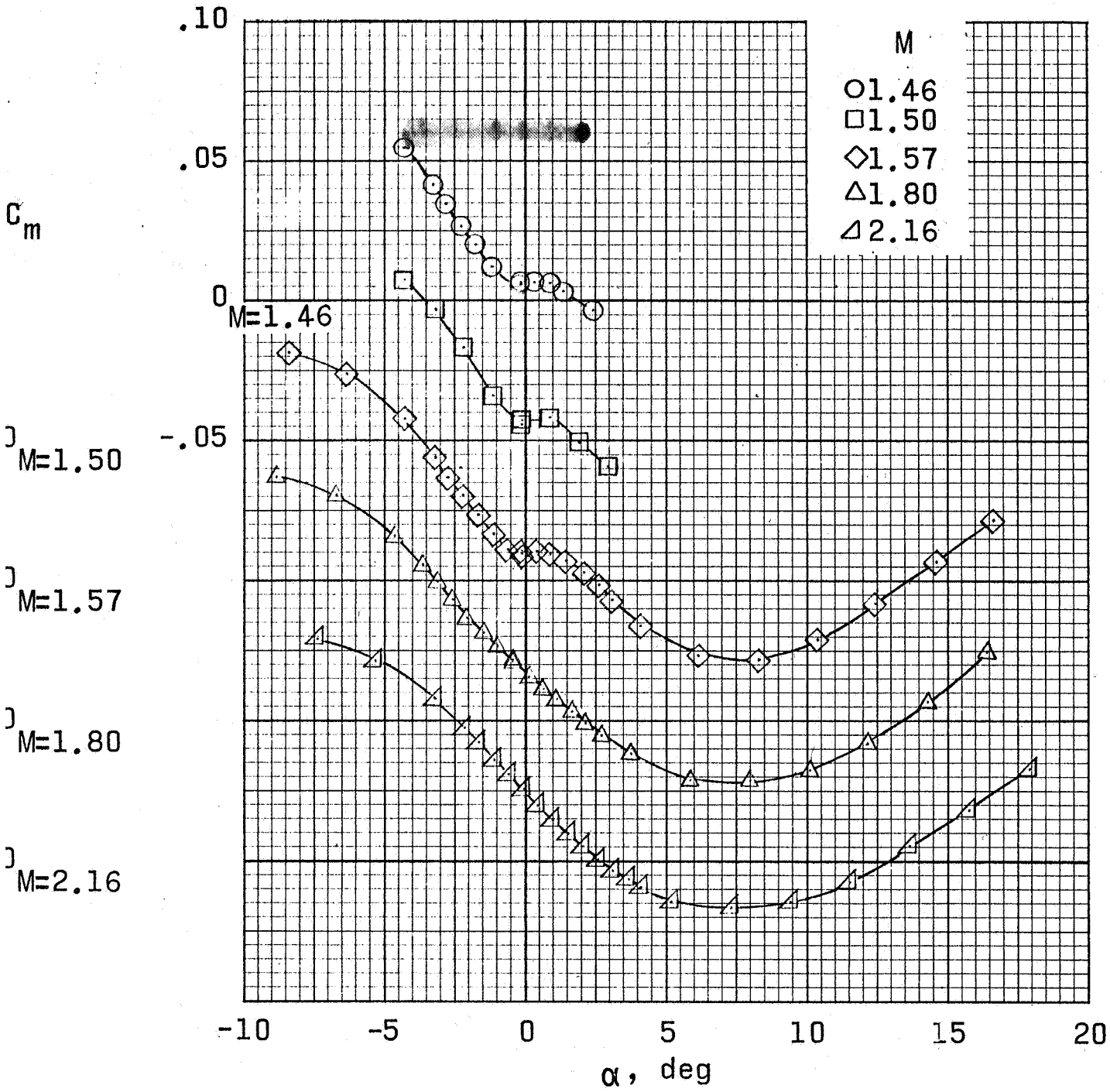

(g) Pitching-moment coefficient.
c.g. = X/D = 0.507 Z/D = 0.0444

Figure 7.- Continued.

[redacted]

[redacted]

[redacted]

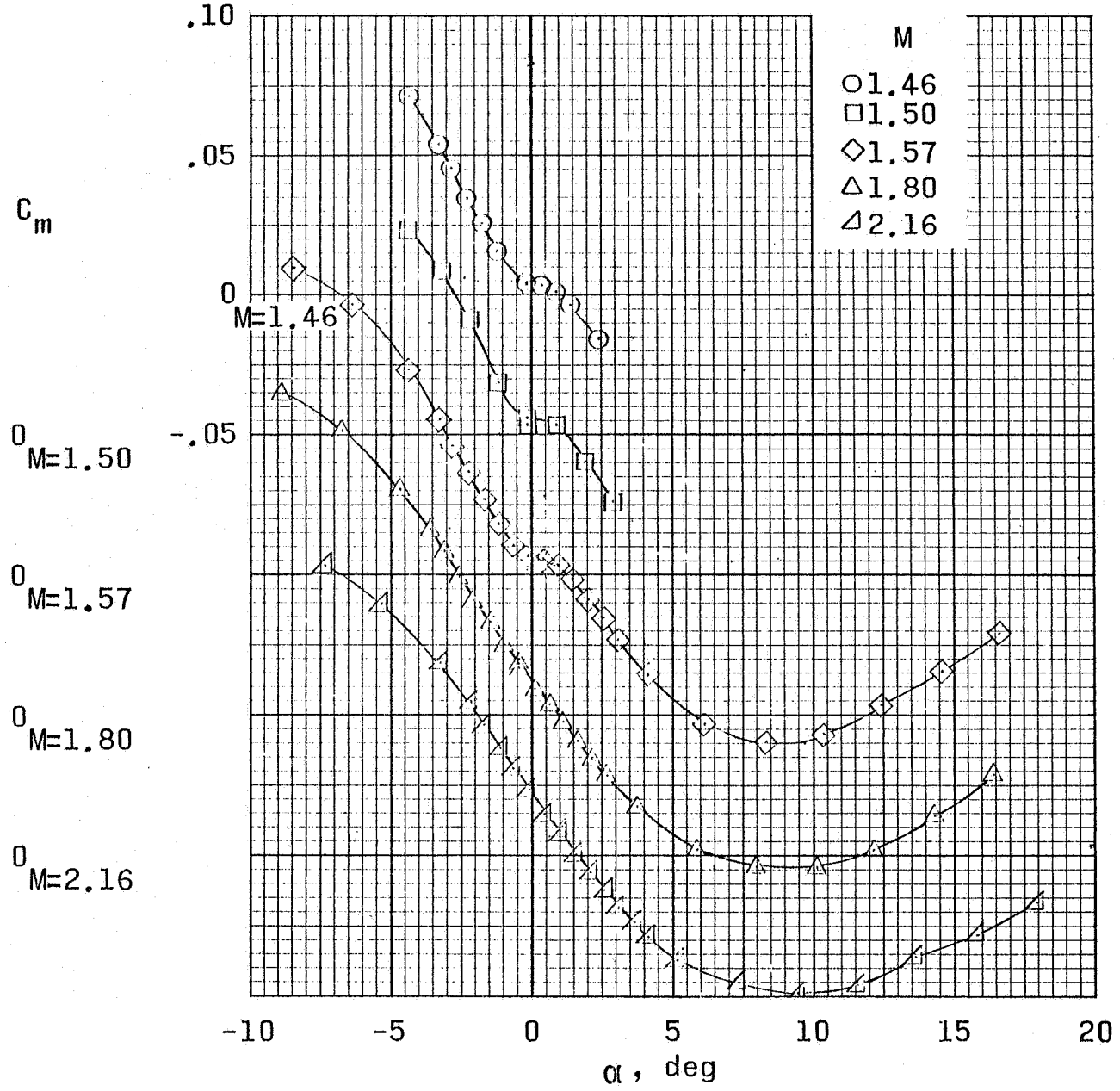

(h) Pitching-moment coefficient.
c.g. = X/D = 0.611 Z/D = 0.0427

Figure 7.- Continued.

[redacted]

[redacted]

[redacted]

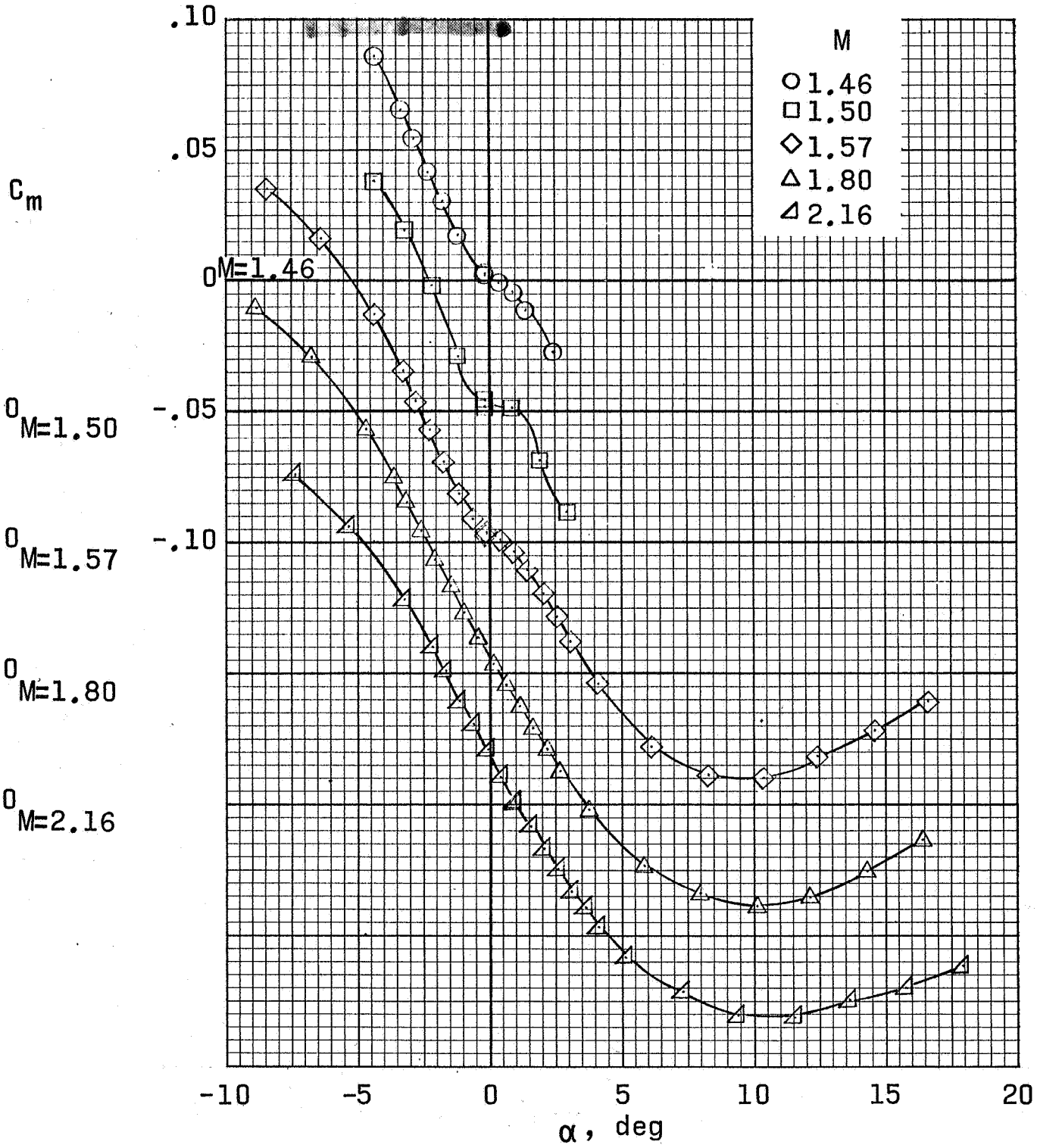

(i) Pitching-moment coefficient.

c.g. = X/D = 0.706 Z/D = 0.0407

Figure 7.- Concluded. [redacted]

[redacted]

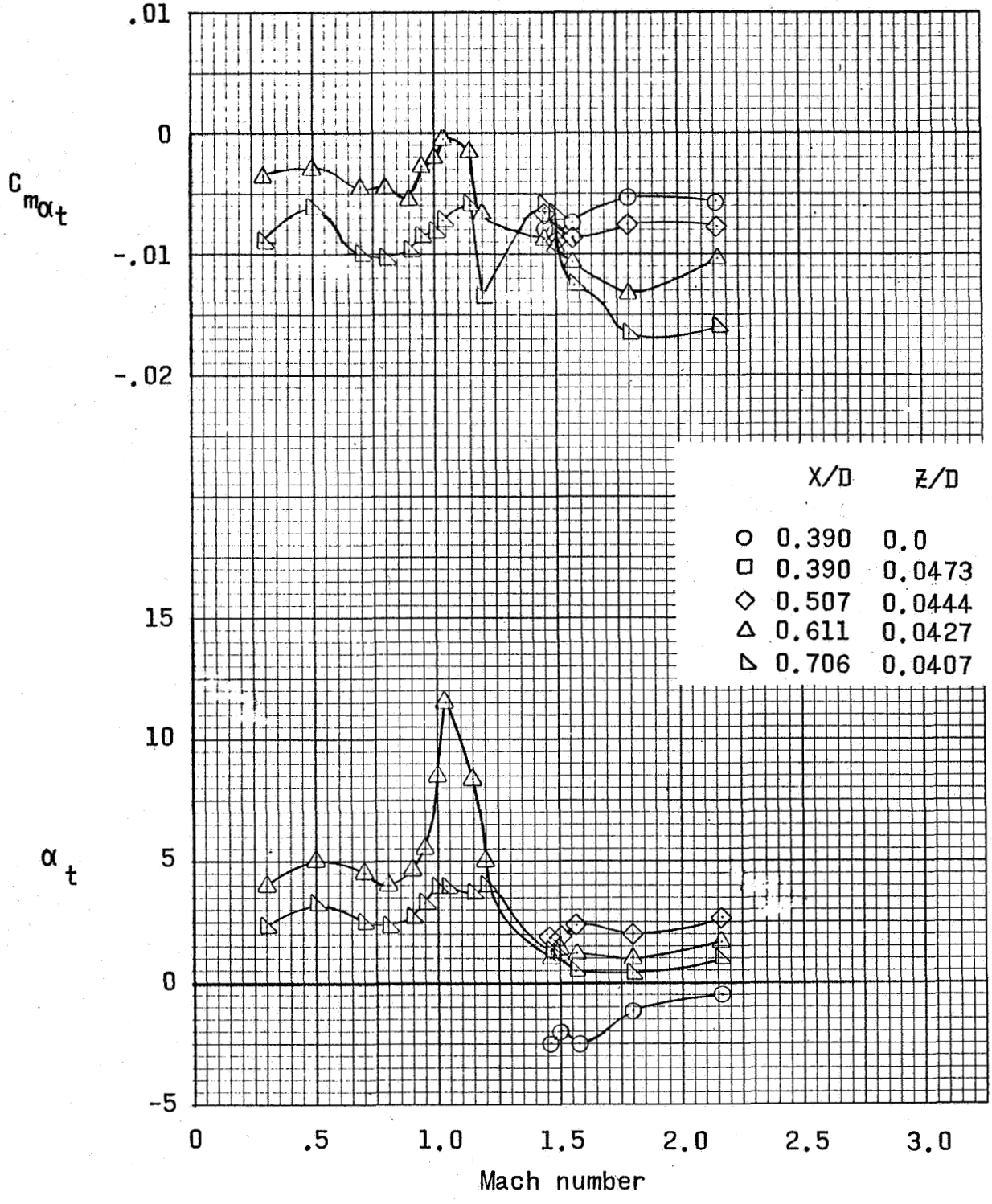

Figure 8.- Effect of cener-of-gravity location of the longitudinal stability characteristics of the atmospheric abort configuration without conical shroud around rocket nozzles.

[redacted]

[redacted]

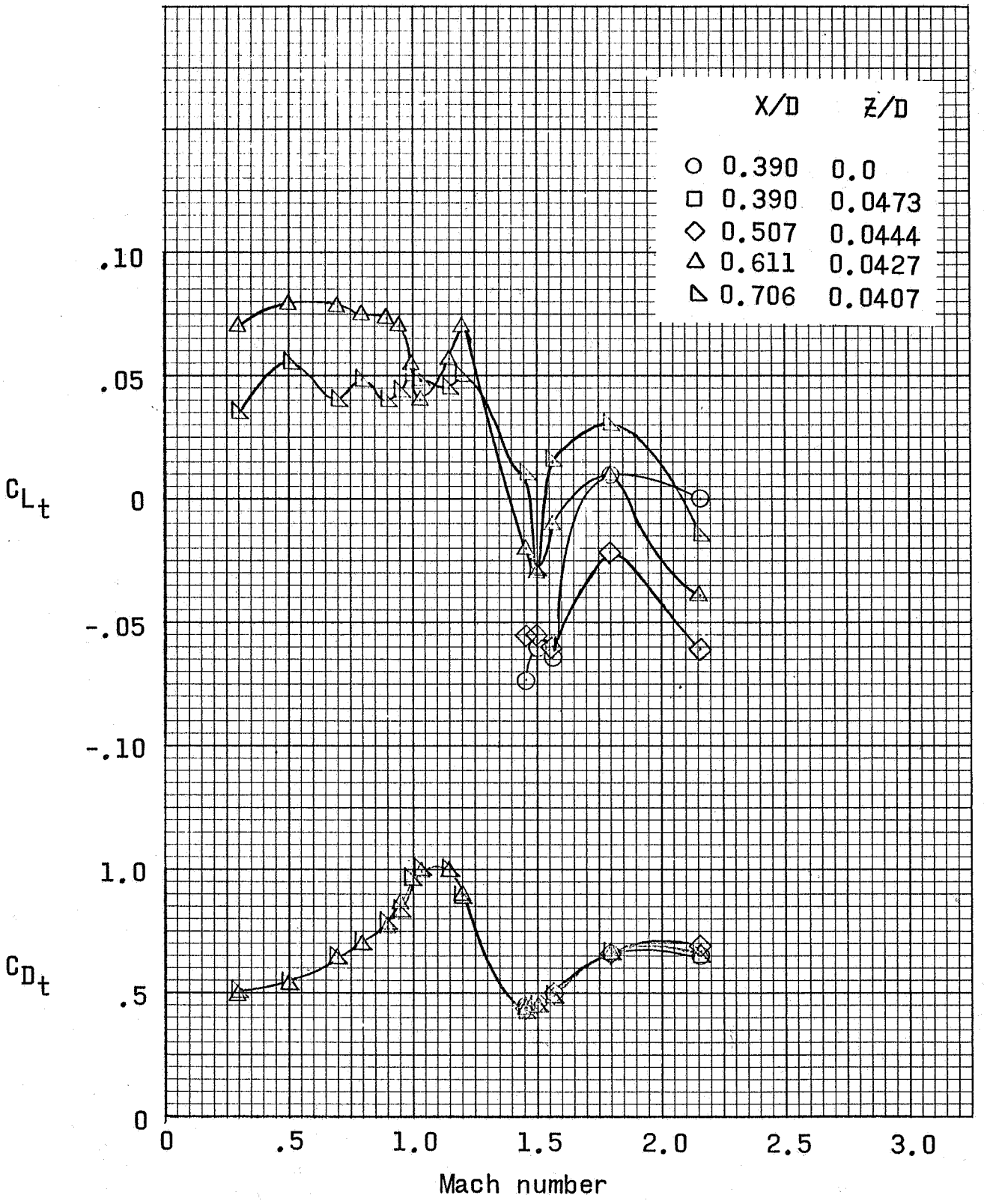

Figure 8.- Concluded.

[redacted]

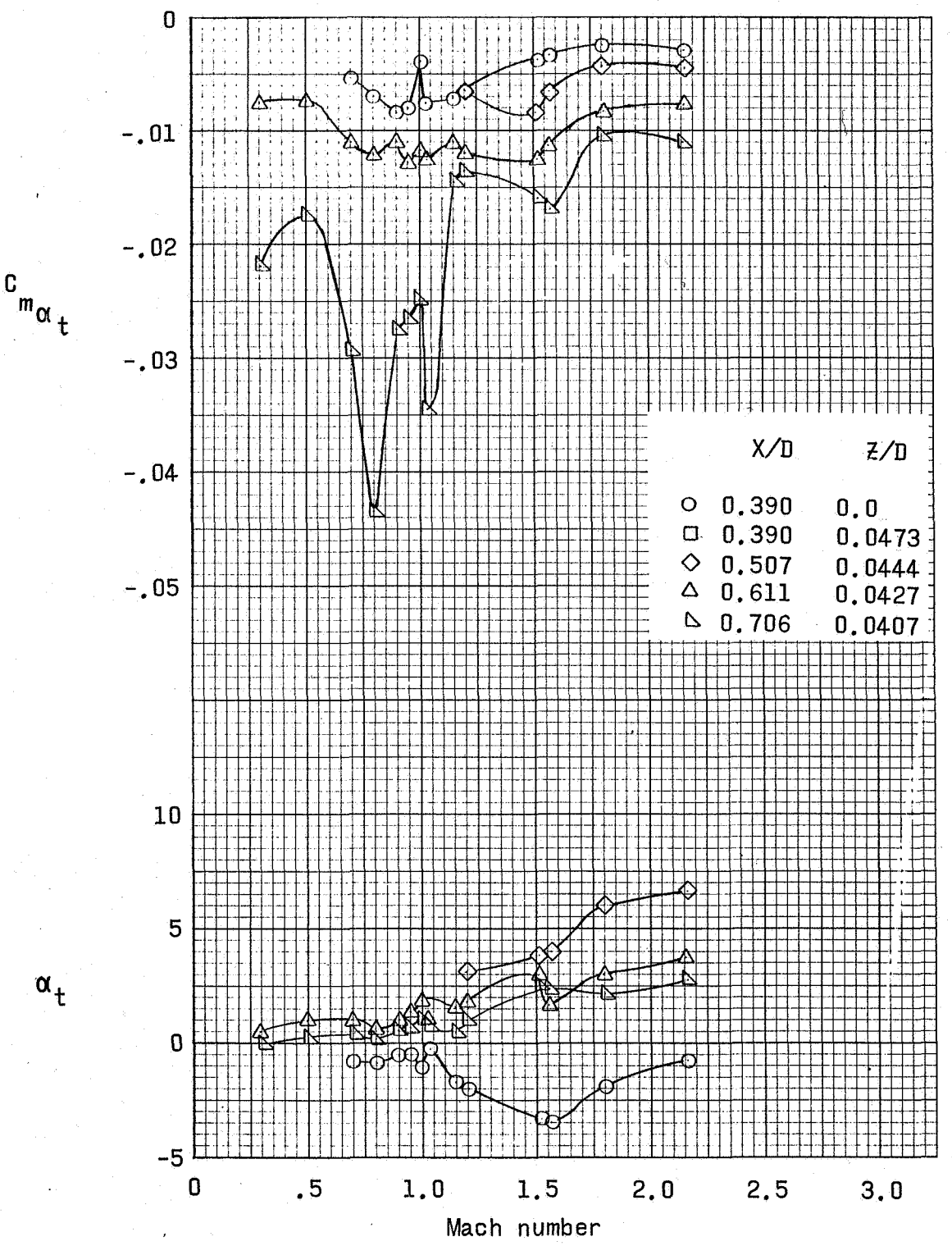

Figure 9.- Effect of center-of-gravity location of the longitudinal stability characteristics of the atmospheric abort configuration with conical shroud around rocket nozzles.

[redacted]

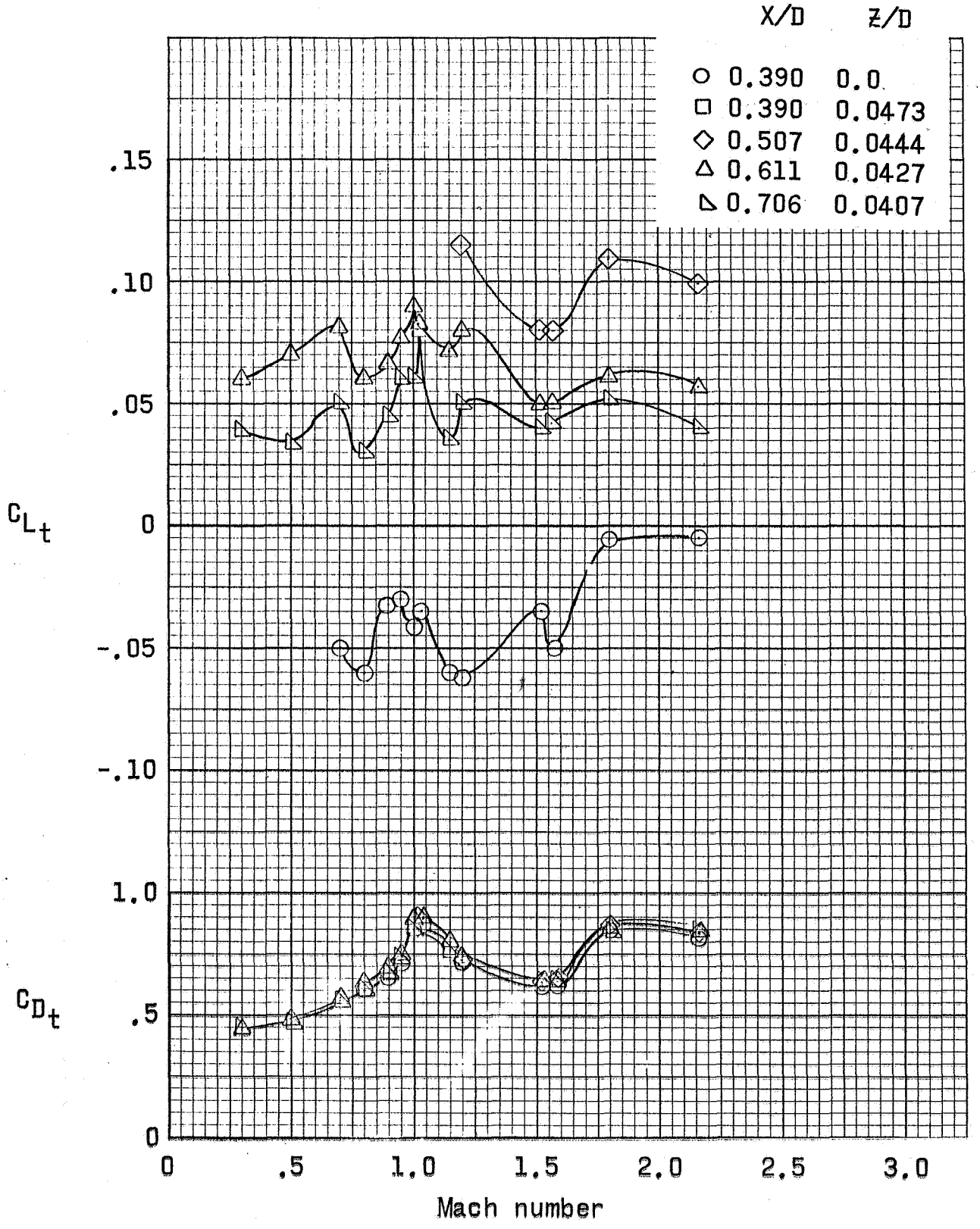

Figure 9.- Concluded.

[redacted]